Survival of the fittest clone: Pro-apoptotic protein Noxa controls selection of lymphocytes under competitive conditions

Wensveen, F.M.

Publication date
2010

CHAPTER IV:

Apoptosis threshold set by Noxa and Mcl-1 regulates competitive selection of T cell clones

Felix M Wensveen[1], Klaas PJM van Gisbergen[1], Ingrid AM Derks[1], Carmen Gerlach[2], Ton NM Schumacher[2], René AW van Lier[1], and Eric Eldering[1]

[1]Department of Experimental Immunology, Academical Medical Center, Amsterdam, The Netherlands
[2]The Division of Immunology, The Netherlands Cancer Institute, Amsterdam, The Netherlands.

Abstract

The adaptive immune system generates protective T cell responses via a poorly understood selection mechanism that favors expansion of clones with optimal affinity for antigen. Here we showed that upon T cell activation, the pro-apoptotic molecule Noxa (encoded by *Pmaip1*) and its antagonist Mcl-1 were induced. During an acute immune response against influenza or ovalbumin, *Pmaip1*$^{-/-}$ effector T cells displayed decreased antigen affinity and functionality. Molecular analysis of influenza-specific T cells revealed persistence of many subdominant clones in the *Pmaip1*$^{-/-}$ effector pool. When competing for low-affinity antigen, *Pmaip1*$^{-/-}$ TCR transgenic T cells had a survival advantage *in vitro*, resulting in increased numbers of effector cells *in vivo*. Mcl-1 protein stability was controlled by T cell receptor (TCR) affinity-dependent interleukin-2 signalling. These results establish a role for apoptosis early during T cell expansion, based on antigen-driven competition and survival of the fittest T cells.

Graphical abstract

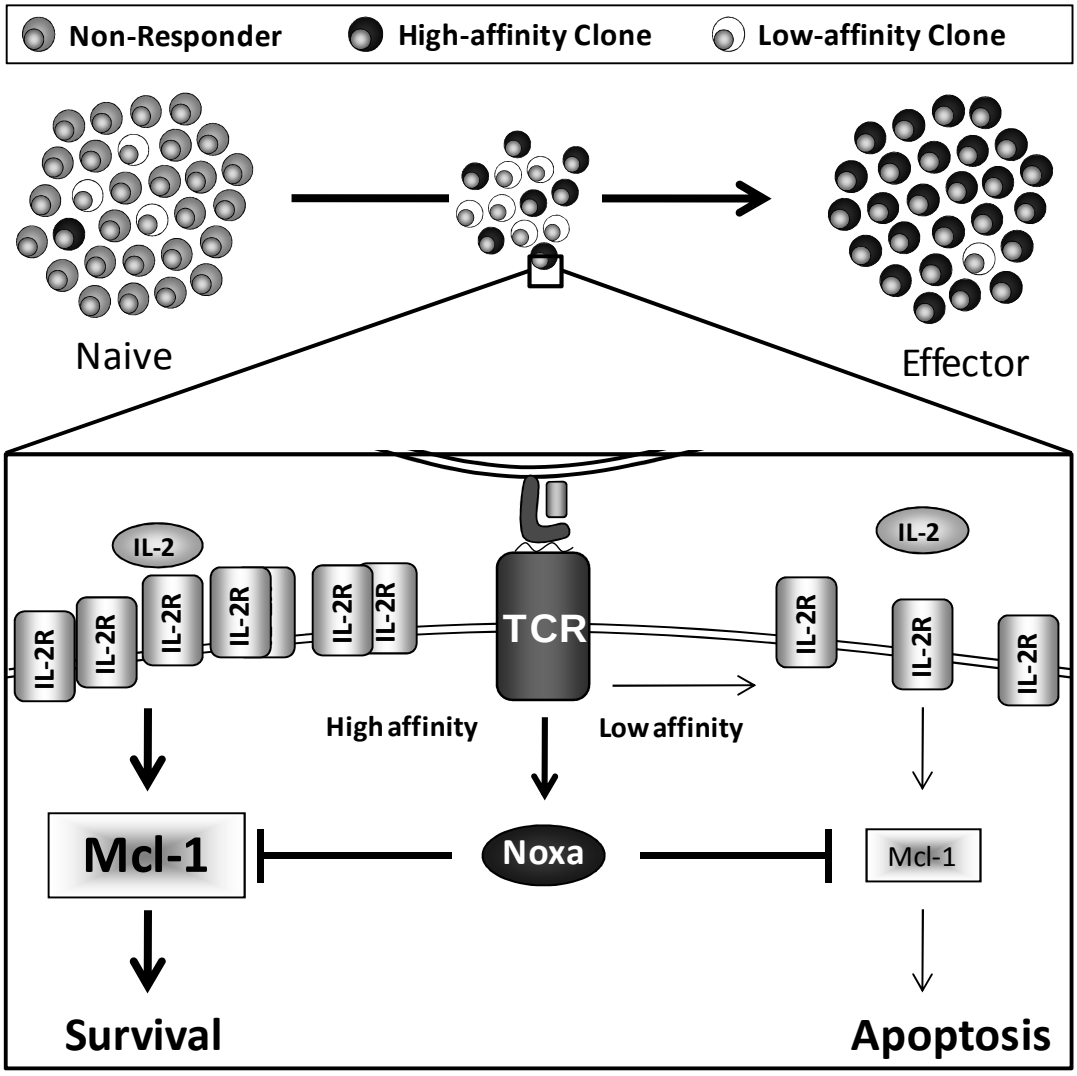

Introduction

Apoptosis plays a central role in T cell immunity by the controlled elimination of cells during selection in the thymus, contraction of the effector pool after antigenic clearance and homeostatic turnover. Upon antigen encounter, high affinity T cell clones are selected and proliferate exponentially from the naïve pool. This crucial step in adaptive immunity has been largely ignored as a phase where apoptosis might contribute to the outcome. Until now, only differences in proliferation have been proposed to be responsible for the dominance of clones with high affinity in effector T cell populations(1,2). Yet, rapid growth creates shifts in selective pressure, which is a basic biological prerequisite for elimination(3). Understanding how apoptosis is controlled or initiated during T cell proliferation would therefore greatly enhance our knowledge on how antigen-specific effector populations are formed.

Apoptosis as a result of cytotoxic stress is mediated by the Bcl-2 family of apoptotic molecules which controls the integrity of the mitochondrial outer membrane. The Bcl-2 family comprises both pro-survival proteins like Bcl-2, Bcl-XL and Mcl-1 and pro-apoptotic BH3-only proteins like Bim, Bid, Puma, Bmf, Noxa and Bad. These two groups of molecules antagonize each other to promote or inhibit the activation of pro-apoptotic Bax-Bak proteins. Upon activation, Bax and/or Bak oligomerize in the mitochondrial outer membrane, thus generating pores through which factors like cytochrome C are released. Once in the cytoplasm, cytochrome C can activate initiator caspase-9, followed by effector caspase activation and cell death(4). The exact molecular mechanism via which Bax and Bak oligomerization is initiated by the activity of BH3-only molecules is still under debate (5,6). What is clear is that there is a hierarchy within the BH3- only subfamily in their ability to promote cell death. Potent apoptosis inducers like Bim, (t)Bid and Puma antagonize with distinct affinities all pro-survival Bcl-2 molecules and directly induce mitochondrial outer membrane permeabilization after transfection in embryonic fibroblasts(7-9). Though these three molecules have non-redundant roles in inducing cell death, only mice deficient for Bim suffer from clear defects within the lymphocyte compartment under homeostatic conditions (10-14). However, upon HSV infection, Bim- and Puma-deficient animals accumulate large numbers of virus-specific $CD8^+$ T cells, which are greatly impaired in their contraction after viral clearance(15). Weak inducers of apoptosis, such as Noxa and Bad, are restricted in their binding of pro-survival molecules(7,8) and function as ‘sensitizers’ or ‘indirect activators’ to increase the potency of Bim, (t)Bid and Puma(16). Mice deficient for ‘sensitizers’ or ‘indirect activators’ generally lack an overt phenotype(17-21). An unresolved issue is whether this is due to redundancy, or weak activity, or that the required conditions for their function have not yet been uncovered.

Activation and subsequent proliferation of T cells induces a radical shift in their metabolic requirements. Survival of cells during this transition is mediated by upregulation of cytokine receptors, such as the interleukin-2 receptor (IL-2R and IL-15R as well as of pro-survival Bcl-2 molecules, such as Bcl-XL. In addition, the availability of pro-survival cytokines like IL-2 in this stage can directly influence the equilibrium between pro- and anti-apoptotic Bcl-2 molecules (22). Previously, we established that naïve human T cells after antigen receptor stimulation *in vitro* upregulate the pro-apoptotic sensitizer Noxa (PMAIP1)(23), originally described as a p53-responsive gene(17) that preferentially interacts with the pro-survival protein Mcl-1 (7-9). Noxa gene targeting provided a survival advantage

for primary and leukemic T cells under conditions of competition for nutrients(24). We have suggested a role for the Noxa-Mcl-1 axis during exponential growth shortly after T cell activation when availability of nutrients and cytokines may be limiting among lymphocytes competing for immunological space (25).

Here, we have elucidated the role of Noxa (encoded by *Pmaip1*) in *in vitro and in vivo* models for T cell activation. The timing of Noxa expression after T cell stimulation correlated with changes in association between Mcl-1 and Bim. Upon acute infection, *Pmaip1*$^{-/-}$ mice showed persistence of subdominant T cell clones, resulting in a more clonally diverse and less efficient effector T cell population. In a model for polyclonal, T cell receptor (TCR)-affinity dependent T cell activation, Noxa deficient T cells generated a larger effector cell response. Upon adoptive transfer into wild-type (WT) mice, Noxa-deficient TCR-transgenic T cells expanded more effectively after low affinity triggering. *In vitro*, antigen affinity determined the expression of the IL-2 receptor, and IL-2 signals controlled the stability of Mcl-1, thus providing high-affinity T cells with a survival advantage. Thus, our results identify apoptosis, mediated by the dynamic balance between Mcl-1, Bim and Noxa, as a key mechanism for the selection of high-affinity T cells during clonal expansion.

Results

TCR ligation shifts the equilibrium between Mcl-1, Bim and Noxa

We screened 40 apoptosis genes for differential regulation after T cell activation by multiplex ligation-dependent probe amplification RT-MLPA(26), using a newly developed murine probeset. Murine CD8^{+} T cells were stimulated *in vitro* with CD3 mAbs alone or combined with CD28 co-stimulation to specify the effects of TCR ligation and co-stimulation. No major differences in transcriptional regulation were observed for these genes between cells with or without CD28 co-stimulation. Direct targets of nuclear factor kappa-light-chain-enhancer of activated B cells (NF-κB)(27), such as the pro-survival molecules Bcl-XL and A1, were rapidly induced after activation (**Figure 1a**, **Figure S1a,b**). Analogous to the human situation, of the BH3-only molecules only Noxa transcripts were increased persistently. In *p53*$^{-/-}$ cells Noxa was upregulated following TCR stimulation, but not γ-irradiation (**Figure 1b** and data not shown), demonstrating that also in mice Noxa transcription after TCR stimulation is independent of p53.

Pro-survival Mcl-1, a major binding partner for Noxa, is most notably regulated on a post-translational level (28,29) and its degradation is instigated after binding to Noxa (30,31). Mcl-1 mRNA amount was not greatly affected by T-cell activation. On a protein level, however, stabilization of Mcl-1 occurred rapidly after TCR triggering, as previously reported (31). Three to five days after T cell activation, Mcl-1 protein gradually decreased (**Figure 1c**; **Figure S1c**), which coincided with Noxa induction on day three after activation.

Previously it has been shown that Noxa and Bim can compete for binding to Mcl-1 (8). Upregulation of Noxa in activated T cells may therefore result in a reduced amount of Bim bound to Mcl-1. Since antibodies against murine Noxa are not available, interactions of Mcl-1 and Noxa cannot be studied directly. Therefore, interactions between Mcl-1 and Bim were compared in wild type and Noxa deficient cells in a semi-quantitative fashion by co-immunoprecipitation following T cell activation. Noxa deficient cells responded similarly to

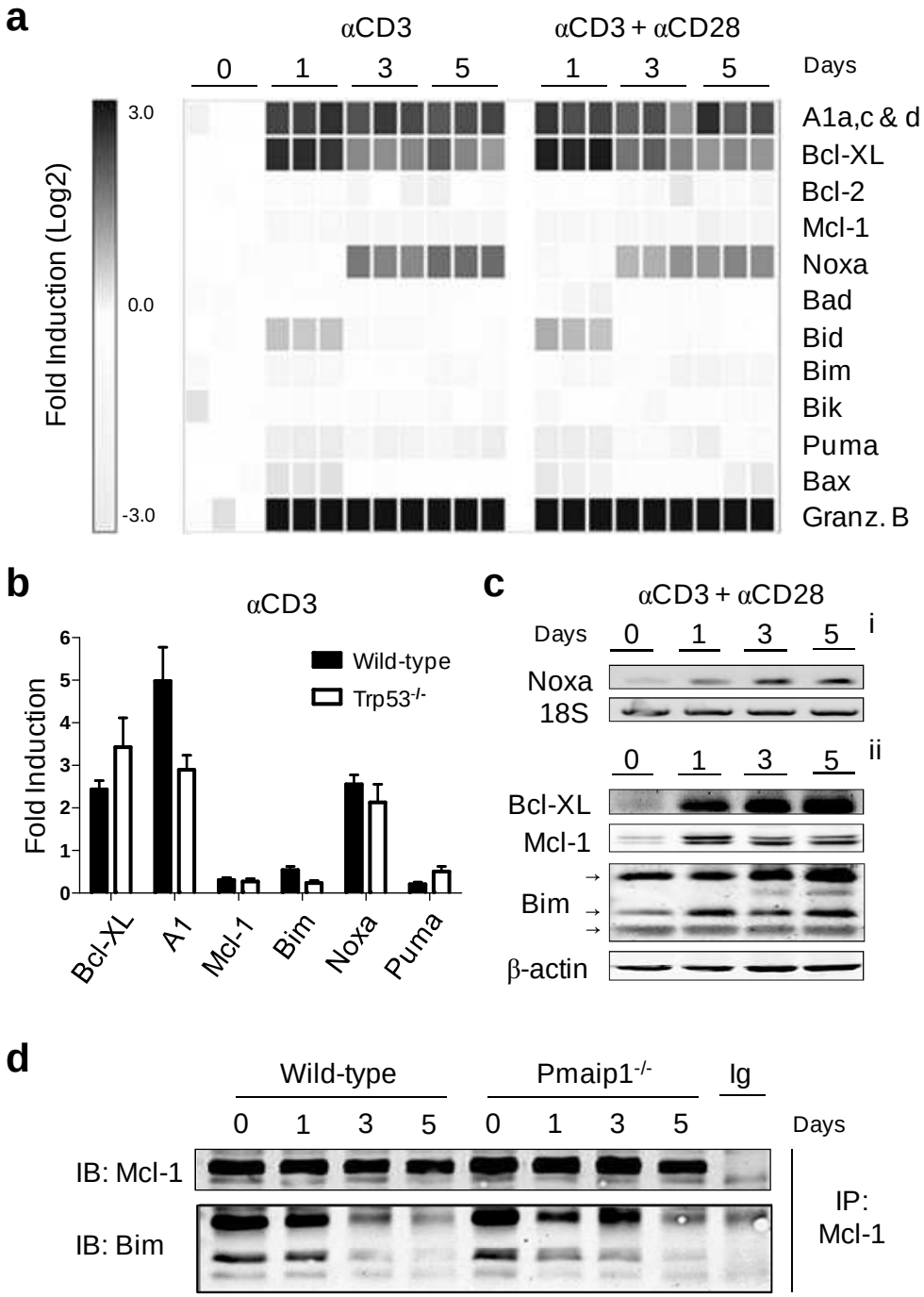

Figure 1. T cell activation leads to a renewed balance of Bcl-2 molecules. (**a**) Expression profiling by RT-MLPA of purified mouse $CD8^+$ T cells after TCR stimulation. Cells were stimulated with solid phase anti-CD3 alone or in combination with soluble anti-CD28. Gene induction of pro- and anti-apoptotic molecules is represented in a heat-map after log transformation of expression levels (scale is from -3.0 to 3.0), relative to averaged values of unstimulated cells at day 0 (n=3). For a color figure, see Appendix III. (**b**) Differential mRNA expression of selected apoptosis regulators in wild-type (WT) (black bars) and *p53*$^{-/-}$ (white bars) $CD8^+$ T cells after five days of anti-CD3 stimulation (n=3). The graph shows means ± s.e.m. (**c**) (i) RT-PCR analysis for Noxa and 18S ribosomal RNA of anti-CD3-anti-CD28 stimulated $CD8^+$ T cells. (ii) Immunoblot analysis of total purified T cells after anti-CD3-anti-CD28 stimulation. A representative result of three independent experiments is shown. (**d**) Immunoprecipitation (IP) of Mcl-1 and immunoblot (IB) for Mcl-1 and Bim in total splenocyte lysates after various days of anti-CD3-anti-CD28 stimulation. For 'day 0' samples twice the amount of protein input was used to compensate for low amounts of Mcl-1. Lane marked "Ig" shows control IP with an irrelevant antibody. One of three experiments with comparable results is shown. Similar findings were obtained using purified T cells. See also Figure S1

in vitro CD3 stimulation as wild type cells and showed no difference in proliferation speed (data not shown). Clearly, Bim became dissociated from Mcl-1 after T cell activation in wild type cells (**Figure 1d**), again coinciding with transcriptional upregulation of Noxa. Moreover, activated T cells from Noxa deficient mice showed prolonged association of Mcl-1 and Bim at day three, implying that Noxa is involved in displacement of Bim from Mcl-1 under these conditions.

Noxa ablation increases memory cell accumulation and naive T cell depletion

The differential regulation of Noxa upon *in vitro* T cell activation and its suggested role in Bim displacement from Mcl-1 prompted us to re-investigate the T cell compartment of Noxa deficient mice. These animals reportedly lack an overt phenotype under homeostatic conditions (17), and extensive analysis of T cell subsets indeed revealed no phenotypic or functional abnormalities in any of the lymphoid organs of young (8-12 wks) Noxa deficient mice (**Figures 2a, b; Figure S2a-f**).

Ageing induces a gradual increase of the effector memory population, which is predominantly caused by antigen exposure (32). Since Noxa is induced upon T cell activation, repetitive cycles of this process *in vivo* might affect the memory T cell compartment in aged (≥ 18 months) Noxa-deficient mice. Clearly, in all investigated lymphoid organs, aged Noxa-deficient mice displayed an increase of the effector memory T cell population, while the naïve T cell pool was concomitantly diminished, most prominently within the $CD8^+$ T cell compartment (**Figures 2c, d; Figure S2g-i**). The central memory population did not appear to be altered in these mice and no indication for auto-reactivity was found by histological examination (data not shown). These data suggested that prolonged and repeated exposure of Noxa-deficient mice to environmental antigens results in augmented recruitment of cells from the naive compartment, leading to effector memory cell accumulation and increased depletion of naive cells.

Ablation of Noxa affects the formation of an oligoclonal effector T-cell population

To investigate whether the observed effector memory cell accumulation in aged Noxa-deficient mice may indeed be caused by an altered response of T cells to antigenic challenge, WT and Noxa deficient mice were infected with the influenza virus A/PR8/34. Phenotypically, $CD8^+$ T cell responses appeared similar between WT and Noxa deficient mice, but both during the expansion and contraction phases there was a small but significant increase in the total number of effector T cells in Noxa deficient animals (**Figure 3a** upper panel and data not shown). Surprisingly, when the antigen-specific population was analyzed qualitatively by tetramer staining, the fraction of T cells specific for the dominant epitope D^b-$NP_{366-374}$, was reduced significantly (**Figure 3a** lower panel) in Noxa-deficient compared to WT mice . This population also bound lower amounts of $D^bNP_{366-374}$ tetramers than WT mice on a per cell basis in all investigated compartments and produced less IFN-γ in response to low peptide concentrations, indicating a reduced TCR affinity and functionality of the effector cell pool (**Figure 3b-d; Figures S3**). Overall TCR expression was not diminished in Noxa-deficient mice (**Figure S3 g,h**), excluding this as the cause for the observed differences.

The effector response against the influenza $NP_{366-374}$ epitope is dominated by one or two high-affinity public $V\beta8.3^+$ clones, with characteristic third complementarity-determining

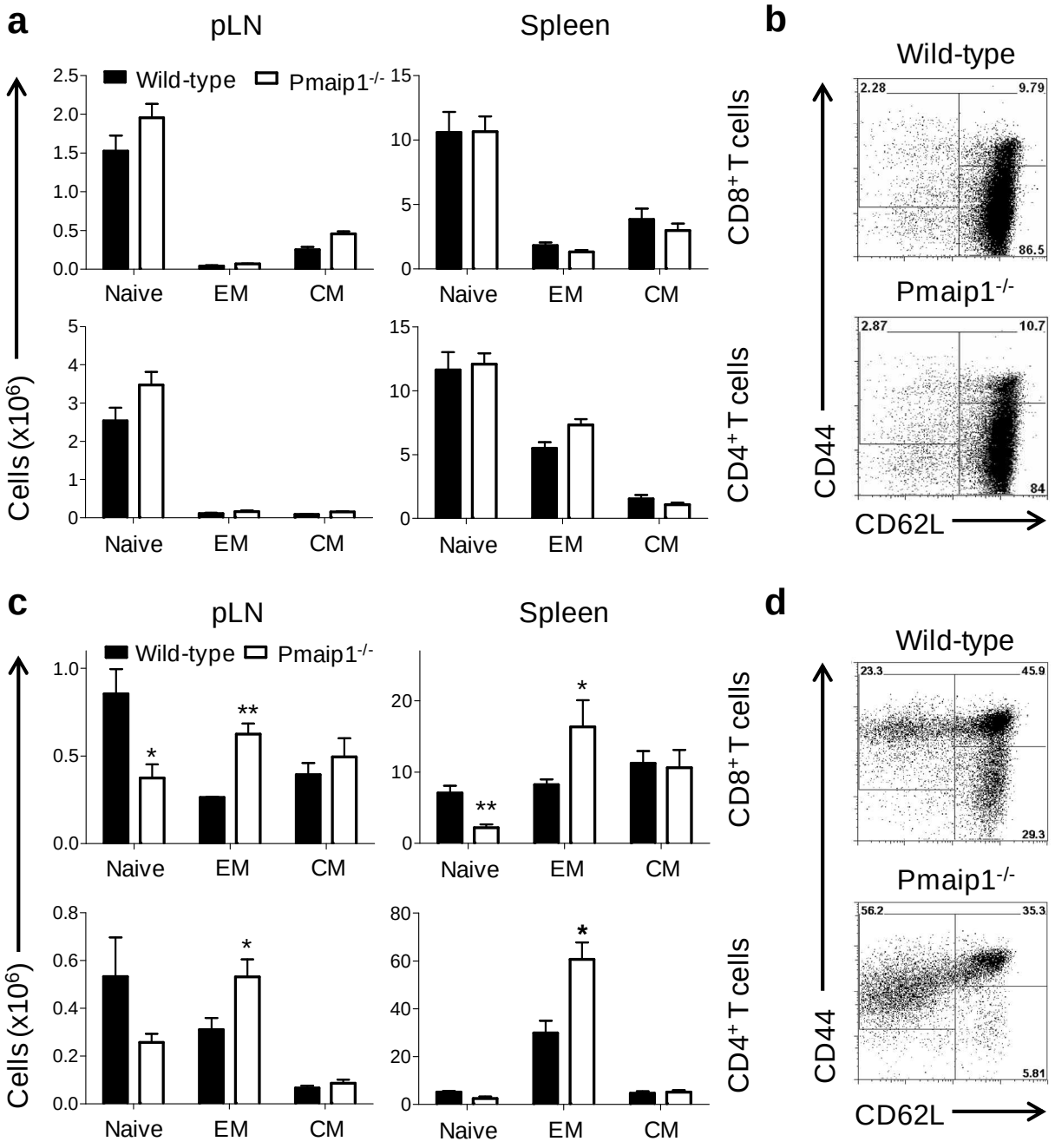

Figure 2. Aged Noxa-deficient mice show accumulation of Effector Memory cells. Wild-type (WT) (black bars) and Noxa-deficient (white bars) mice were maintained under homeostatic conditions for 12 weeks (**a, b**) or 18 months (**c, d**) and analyzed by flow cytometry. (**a,c**) Absolute number of naïve ($CD44^{dim}CD62L^{+}$), effector memory ($CD44^{+}CD62L^{-}$; EM) and central memory ($CD44^{+}CD62L^{+}$; CM) CD8 (Top panels) and CD4 (bottom panels) T cells in peripheral lymph nodes (pLN; left panels) and spleen (right panels) of young (**a**) and aged (**c**) mice are shown. (**b,d**) Representative flow cytometry plots for $CD8^{+}$ T cell subsets in the spleens of young (**b**) and aged (**d**) WT and Noxa-deficient mice. The graphs show means ±s.e.m. Asterisks denote significant differences (* $p<0.05$, ** $p<0.005$). See also Figure S2.

regions CDR3 regions (33). The generation of such a highly restricted response suggests a strong selective process during the formation of the effector T cell population. The influenza model therefore provides a unique opportunity to analyze whether the decreased affinity and function of effector cells in Noxa-deficient mice corresponds with an altered usage of public $V\beta8.3^{+}$ clonotypes. $D^{b}NP_{366-374}$ specific $CD8^{+}$ T cells were purified at the peak of the CTL

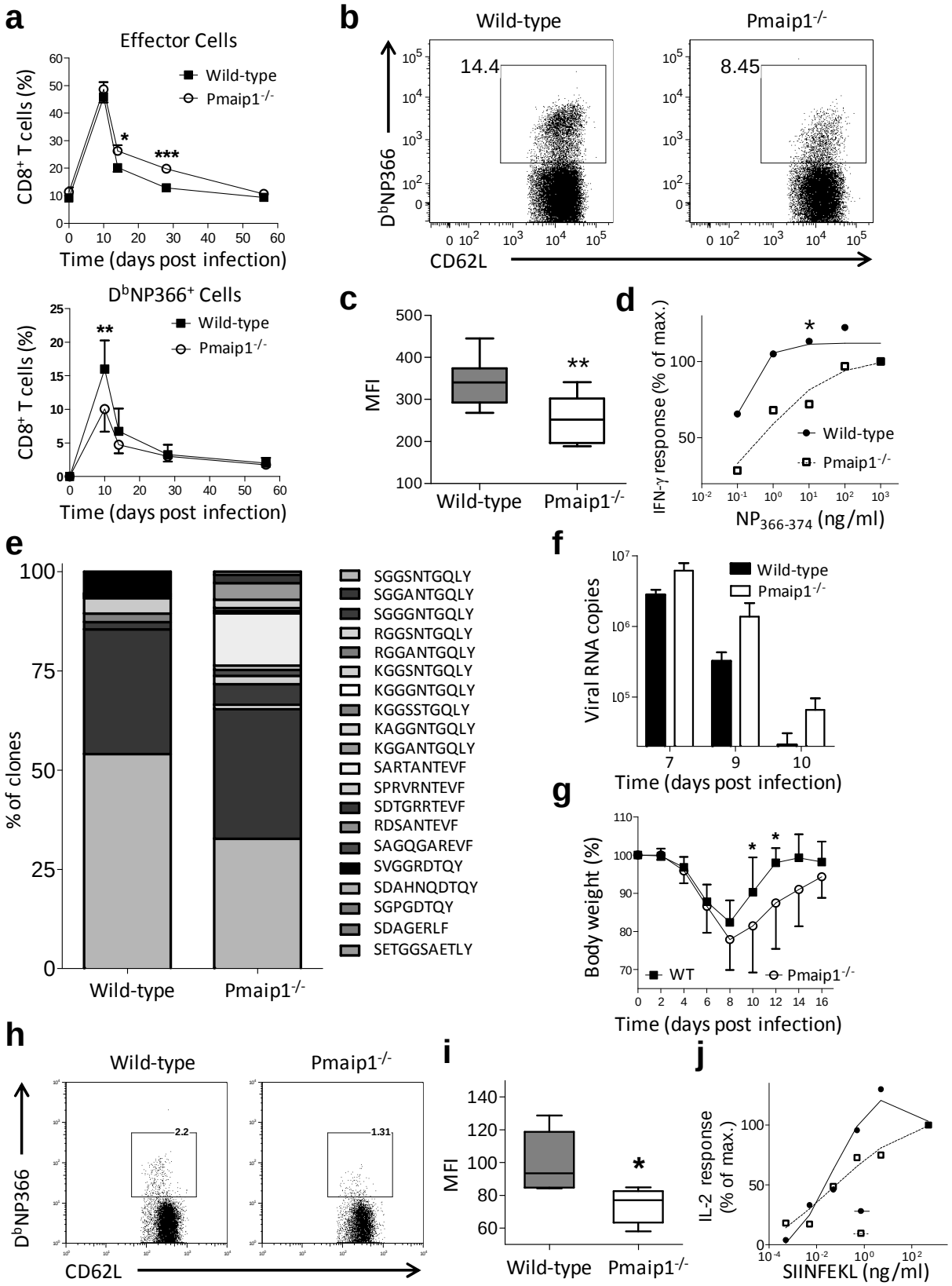

Figure 3. Decreased antigen affinity and increased TCR diversity of antigen specific CD8 T cells in Noxa-deficient mice. (**a**) Total $CD44^+CD62L^-$ effector (Top) and D^bNP366-specific (bottom) $CD8^+$ T cells in the blood of Influenza infected WT (black squares) and Noxa-deficient (*Pmaip1*$^{-/-}$, white circles) mice (n = 8). (**b**) Representative FACS™ plots of $CD8^+$ T cells in the lung, stained with D^bNP366 tetramers. (**c**) Quantification of the mean fluorescence intensity (MFI) of D^bNP366 binding blood $CD8^+$ T cells on day 10 p.i. (**d**) IFNγ production induced by varying doses of peptide in $NP_{366-374}$ re-stimulated splenic $CD8^+$ T cells from influenza infected mice, relative to the level of cells stimulated

with saturating (500 ng/ml) amounts of peptide on day 10 p.i. (**e**) Cumulative clonal composition of the Vβ8.3$^+$NP366$^+$ CD8$^+$ T cell population in WT and Noxa-deficient mice, 10 days p.i. with Influenza virus. Given is the relative contribution of each clone to the total Vβ8.3$^+$NP366$^+$ population (WT n = 182, Noxa-deficient n = 149 clones sequenced from 4 mice of each), amino acid sequence of CD3 regions is indicated. For a color picture, see Appendix III (**f**) Virus titers in influenza infected WT and Noxa-deficient mice at separate days (day 7-10) after infection were measured in the lung (total number of mRNA copies of the viral M_1 matrix gene). Data shown are representative for 2 separate experiments performed using 5-8 mice at each timepoint. (**g**) Body weight of WT and Noxa-deficient mice (n = 8) infected with Influenza virus, relative to their weight at the start of the experiment. Shown are representative data of three independent experiments with comparable results. (**h**) Antigen affinity of specific CD8$^+$ T cells in mice immunized intradermally with a DNA construct encoding SIINFEKL peptide from ovalbumin (OVA). Representative FACS^{TM} plots of CD8$^+$ T cells in the blood, stained with K^{b}OVA. (**i**) Quantification of the mean fluorescence intensity (MFI) of K^{b}OVA binding CD8$^+$ T cells from the experiment in **h** on day 12 p.i. (n=8 for WT and Noxa-deficient mice). (**j**) IL-2 production induced by varying doses of SIINFEKL stimulated CD8$^+$ T cells from intradermally immunized mice, relative to the level of cells stimulated with saturating (500 ng/ml) amounts of peptide. n.s. = not significant. Where applicable, error bars indicate s.e.m. See also Figure S3.

response by FACS^{TM} sorting using stringent gating, and clonal expansion within the Vβ8.3$^+$ positive T cells was confirmed via spectratype analysis (**Figure S3i**). Strikingly, analysis of the D^b-NP$_{366-374}$-specific and Vβ8.3$^+$ CD8$^+$ T cell population at the peak of the CTL response revealed a more diverse set of clonotypes and a smaller contribution of the public dominant clone in Noxa-deficient mice (**Figure 3e**), indicating persistence of subdominant clones. To quantify diversity, the Simpson's Diversity index (SDI) was used, previously described as the best method to compare the diversity of TCR repertoires (34). This 0 to 1 scale describes the chance of finding two different clones when two clones of a single sample are analyzed, with a value of 1 representing maximum diversity. An SDI of 0.34 and 0.61 was calculated for WT and Noxa-deficient clones respectively, indicating that Noxa-deficient mice generate a clonally much more diverse effector cell pool upon Influenza infection.

Previously, it has been demonstrated that the affinity of several of these clones is reduced compared to the dominant clonotype (35)**.** The suboptimal response against a single, well-characterized epitope correlated with increased pathogenicity as determined by delayed viral clearance and by slower recovery from bodyweight loss in Noxa-deficient versus WT mice (**Figures 3f,g**). Thus, it appears that Noxa does not regulate the maximum overall effector population size, but plays a role in the selective outgrowth of optimal T cell clones by contributing to apoptosis of subdominant clones.

Differences in viral load may lead to altered T cell responses (36). To establish the impact of Noxa on CD8$^+$ T effector cell selection independent of pathogenic load, we analyzed effector responses in a second acute T cell activation model, using a pathogen-free immunization strategy. Mice were immunized via intradermal DNA-tattooing (37) with constructs encoding an ovalbumin-derived peptide (SIINFEKL) fused to a tetanus toxin fragment. Also in this response, tetramer binding affinity and the cytokine response upon restimulation in vitro with OVA-peptides was reduced in Noxa-deficient compared to WT effector T cells (**Figure 3h-j**). K^b-SIINFEKL specific responses are enriched for Vβ5.2 positive cells (1). Molecular analyses of sorted clones of wild type mice revealed that in this case, TCR diversity within the Vβ5.2$^+$ family (1) of K^b-SIINFEKL positive cells was large and not restricted to one dominant public clone. The decreased affinity of Noxa-deficient clones was therefore not manifest against this background of a 'private' and already highly

diverse (SDI > 0.66) WT TCR repertoire (Figure S3j). Together these data indicate that the effects of Noxa depend on affinity of the TCR for MHC-peptide, as revealed by decreased functionality of effector cells, and increased CDR3 diversity in the sequence space surrounding dominant clones.

No overt differences in the naïve T cell compartment between WT and Noxa-deficient mice

The observed differences in Noxa-deficient T cell responses after Influenza infection may originate from differences in the naïve T cell repertoire, caused by altered thymic selection. However, thymocytes and naïve T cells from Noxa-deficient mice were phenotypically and functionally indistinguishable from their wild type counterparts (**Figure 4a** top and middle). Apoptosis of CD4-CD8 double positive (DP) thymocytes as a result of

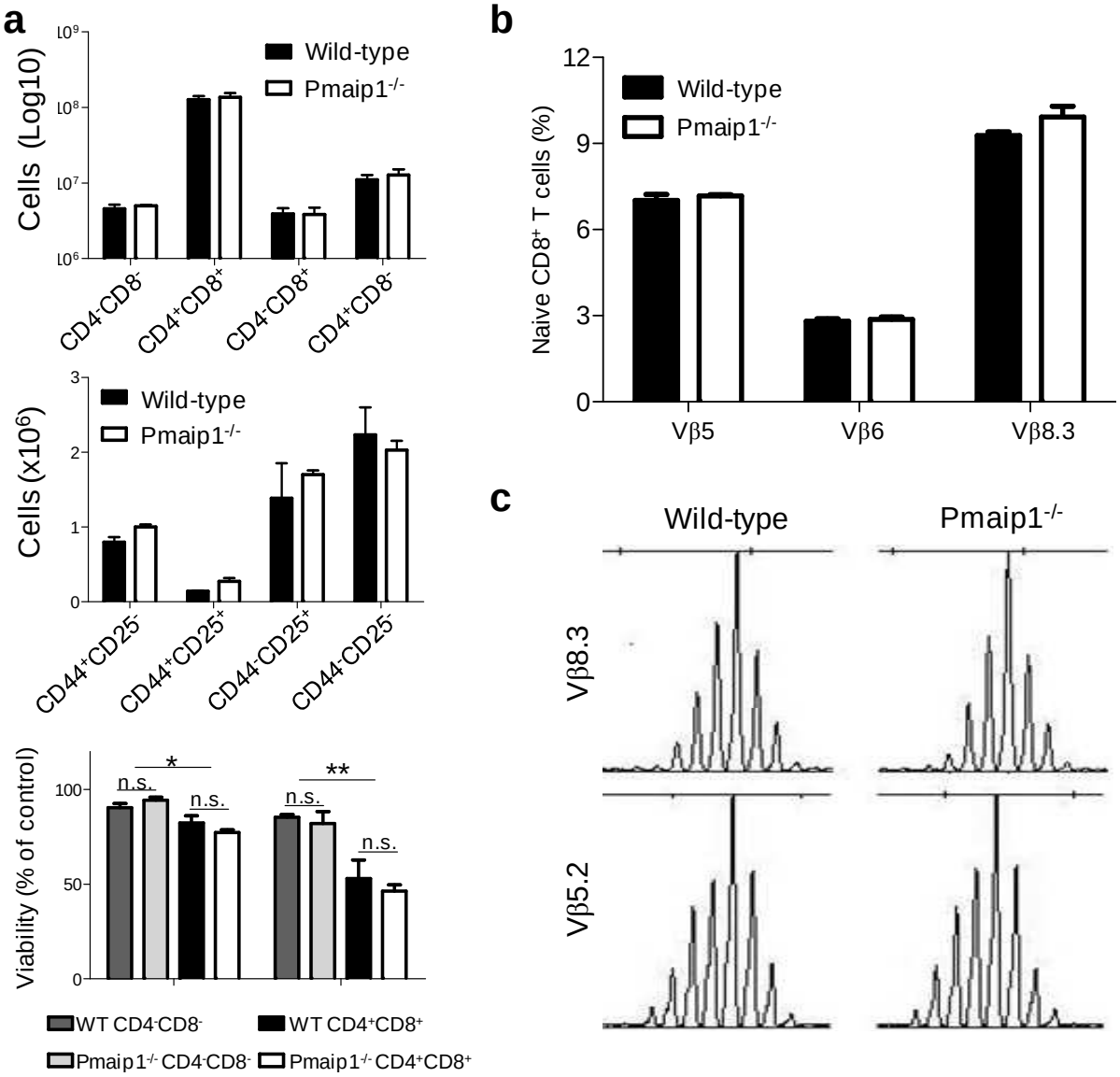

Figure 4. Noxa-deficient mice show no signs of altered thymic selection. (**a**) Absolute numbers of total (top) and $CD4^-CD8^-$ (middle) thymocyte subsets. (bottom) Thymocytes were stimulated in vitro with solid phase anti-CD3 and viability was assessed by AnnexinV-To-Pro-3 staining. (**b**) Phenotyping of peripheral $CD8^+$ T cells reveals a normal distribution of TCR Vβ usage in Noxa-deficient mice. Error bars indicate s.e.m. (**c**) Spectratype analysis of naive $V\beta5.2^+$ and $V\beta8.3^+$ $CD8^+$ T cells in Wild Type and Noxa-deficient mice.

stimulation with CD3 mAbs *in vitro* is prevented in Bim-deficient mice, showing that Bim plays an important role in negative thymic selection (38). Anti-CD3 antibodies had no influence on survival of CD4-D8 double negative cells, but rapidly induced apoptosis in DP cells (**Figure 4a** bottom). No survival advantage was seen for Noxa deficient cells. Expression of Noxa was undetectable in thymocytes, in contrast to Bim which is highly expressed in DP cells. TCR triggering in these cells also did not lead to Noxa induction (data not shown).

Next, peripheral naïve T cells were compared for TCR Vβ usage and CDR3 length distribution. No differences between WT and Noxa-deficient mice were seen in the amount of naïve ($CD44^{dim}CD62L^{+}$) CD8 T cells expressing Vβ5, Vβ6 or Vβ8.3 (**Figure 4b**). Spectratype analysis of flow sorted naïve cells revealed a normal Gaussian distribution with no increase of exceptionally short or long sequences within the CDR3 regions of the Vβ5.2 and Vβ8.3 families of Noxa-deficient mice (**Figure 4c**). These findings show that Noxa-deficient mice have a normal naïve T cell repertoire of similar composition as wild type mice, and suggest that the observed differences in acute activation models therefore most likely arise after peripheral activation by antigen.

Noxa ablation allows enhanced expansion of T cells upon low-affinity triggering

In order to establish whether the observed differences in clonal selection were intrinsic to T cells and based on the affinity of TCR triggering, several approaches were taken. First, we reasoned that activation independent of TCR affinity should induce no differences in expansion between WT and Noxa-deficient mice. In support of this notion, the superantigen staphylococcal enterotoxin B (SEB), which activates all $V\beta8^{+}$ T cells independent of their antigen-specificity (39), elicited $CD4^{+}$ and $CD8^{+}$ T cell responses of similar magnitude in WT and Noxa deficient animals (**Figure 5a,b**).

Second, we investigated whether the observed phenotype was T cell intrinsic. An adoptive transfer system was used of abundant T cell co-stimulation, in which vast polyclonal T cell expansion based on antigen recognition occurs. Mice that constitutively express the TNFRFS7 (CD27) ligand CD70 on B cells ($CD70^{TG}$ mice) possess an enlarged fraction of effector T cells, which is dependent on environmental antigen recognition (40-42). WT or Noxa-deficient ($Ly5.1^{+}$) T cells were transferred into CD27-deficient or CD27-deficient-$CD70^{TG}$ ($Ly5.2^{+}$) mice. These recipients have no overt phenotype and only the donor T cells can respond to the CD70 transgene, since they express CD27. In this milieu of continuous CD70 co-stimulation, transferred T cells underwent rapid expansion, which was significantly larger after transfer of Noxa-deficient T cells (**Figure 5c**). The majority of cells upregulated the effector cell marker KLRG1 (43), indicating that these cells originated from a recently activated precursor. (**Figure 5d, Figure S4**). At three weeks after transfer the expanded population had undergone almost complete contraction, indicating that the antigen-responsive pool of transferred naïve clones, required to supplement and thus maintain the short lived effector cell population, had been depleted. The contraction of donor effector cells occurred with similar kinetics between wild type and Noxa-deficient cells, suggesting that this phase is independent of Noxa in this model.

Third, to gather formal proof that Noxa ablation provides an *in vivo* advantage over Noxa sufficient cells in a TCR affinity dependent fashion, Noxa-deficient mice were crossed

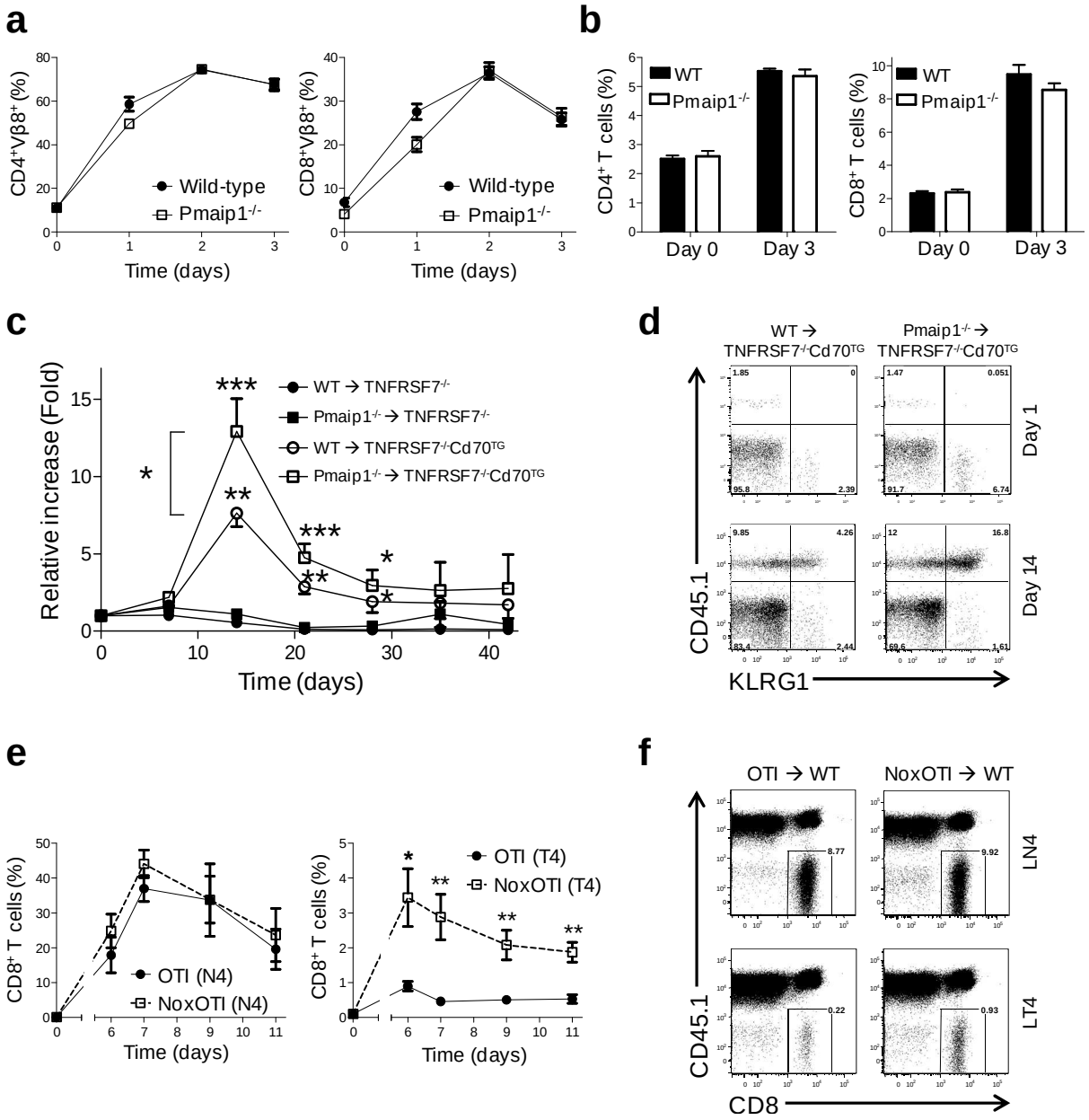

Figure 5. Noxa ablation provides a T cell intrinsic, TCR-affinity dependent competitive survival advantage for low-affinity T cells. a,b, Mice were injected intraperitoneally with 20ug Staphylococcal Enterotoxin B (SEB) and Vβ8-positive T cell responses were analyzed by flow cytometry. (**a**) Relative increase of $CD4^+$ (left) and $CD8^+$ (right) effector cells within the Vβ8 positive fractions. (**b**) Relative number of Vβ8 positive $CD4^+$ (left) and $CD8^+$ (right) T cells as a fraction of total $CD4^+$ and $CD8^+$ cells respectively **c,d,** Increased expansion of Noxa-deficient donor cells after transfer to a $CD70^{TG}$ host. (**c**) WT (Wt→) and Noxa-deficient (*Pmaip1*$^{-/-}$→) T cells ($Ly5.1^+$) were adoptively transferred in CD27-deficient ($TNFRSF7^{-/-}$) or CD27-deficient-$CD70^{TG}$ recipient mice ($Ly5.2^+$). Shown is the increase of donor $CD8^+$ T cells in the blood as a fraction of the total number of $CD8^+$ T cells, relative to day 1 (N=5). Statistical differences are compared to wt cells transferred to CD27-deficient recipients, unless indicated otherwise (**d**) Phenotypic analysis of adoptively transferred cells by KLRG1 staining. Cells were gated for $CD8^+$ T cells. **e, f**, OT-I and NoxOTI T cells ($Ly5.2^+$) were adoptively transferred in Wild Type recipient mice ($Ly5.1^+$). One day after transfer, recipient mice were infected with Listeria-SIINFEKL (LN4; n=3) or with Listeria SIITFEKL (LT4; n=5) One mouse transferred with OT-I T cells was poorly infected with LN4 and was excluded from the analysis. (**e**) Shown is the number of donor cells as a fraction of the total CD8 T cell pool. (**f**), Representative FACS^{TM} plots of total white blood cells 6 days after infection. See also Figure S4 where data from a replicate experiment are shown. Where applicable, error bars indicate s.e.m.

with OT-I TCR transgenic mice. Low amounts of purified $CD8^+$ T cells from these Noxa-deficient /OT-I (termed NoxOTI here) mice or from conventional OT-I mice (both $Ly5.2^+$) were transferred to WT recipients ($Ly5.1^+$), to provide sufficient competition of the transferred cells with the host response after immune activation. One day after transfer, mice were infected with a *Listeria monocytogenes* strain expressing the high-affinity peptide SIINFEKL (LN4), or the low-affinity peptide SIITFEKL (LT4) (1), and T cell responses were followed in the blood. For mice infected with LN4, there was no significant difference between OT-I and NoxOTI T cells which both expanded to approximately 40% of total effector cells at the peak of the response (**Figure 5e**). As expected (1), infection with LT4 provided a highly reduced response, which reached its maximum one day earlier. Significantly, transferred NoxOTI cells showed a response which expanded up to four times the amount of transferred OT-I cells (**Figure 5e**). Representative FACS™ staining and additional data from two separate transfer experiments is shown in **Figures 5f** and **S4b, c**.

Combined, these transfer experiments indicate that specifically after low-affinity TCR stimulation, Noxa ablation provides an intrinsic selective advantage for expanding T cells *in vivo*.

Affinity of TCR ligation controls Mcl-1 stability

The involvement of Noxa in formation of high-affinity effector populations implies that the affinity of the TCR-ligand interaction influences the balance between Noxa and its binding partners. To test this directly, the effect of TCR binding affinity on the regulation of Bcl-2 members on a transcriptional and post-translational level was investigated. OT-I transgenic T cells were stimulated *in vitro* for 5 days with high (SIINFEKL; N4), intermediate (SAINFEKL; A2), or low (SIITFEKL; T4, SIIQFEKL, Q4) affinity peptides (1). No differences in the transcriptional regulation of the Bcl-2 molecules, including Mcl-1, A1, Bim and Noxa was observed between cells stimulated with N4 or A2. However, on a protein level, after the initial induction (see also Figure 1c), Mcl-1 declined more rapidly under conditions of suboptimal stimulation, while amounts of Bim and Bcl-XL remained constant (**Figure 6a, Figure S5c**). No significant differences in proliferation were observed between N4 and A2 peptides. In contrast, stimulation with lower-affinity peptide resulted in a lower induction of CD25, the α chain of the IL-2 receptor (**Figure 6b**). IL-2 and IL-15 share the usage of their β-chain and of the common γ chain (γ_c) , and signaling through γ_c-receptors has previously been associated with Mcl-1 stability as well as with Bim- and Noxa-mediated survival (22,44). CD25 expression was clearly associated with the dose and affinity of peptides used to stimulate OT-I T cells (**Figure S5b**). To establish whether IL-2 signaling regulated Mcl-1 expression, OT-I T cells were stimulated in vitro with limiting N4 or T4 peptide in the presence or absence of exogenous IL-2. Low dose T4 stimulation provided poor T cell activation with significantly less CD25 expression than after N4 stimulation. T4 stimulation in the presence of exogenous IL-2, on the other hand, boosted CD25 expression to the level observed after N4 stimulation alone (**Figure 6c-i**). Addition of 10ng/ml IL-2 alone did not induce T cell activation or CD25 expression. Western blot analysis revealed that Mcl-1 amounts correlated strongly with CD25 expression (**Figure 6c-ii**), suggesting that TCR affinity mediates cellular survival indirectly via differential IL-2R signaling and regulation of the Noxa-Mcl-1 axis.

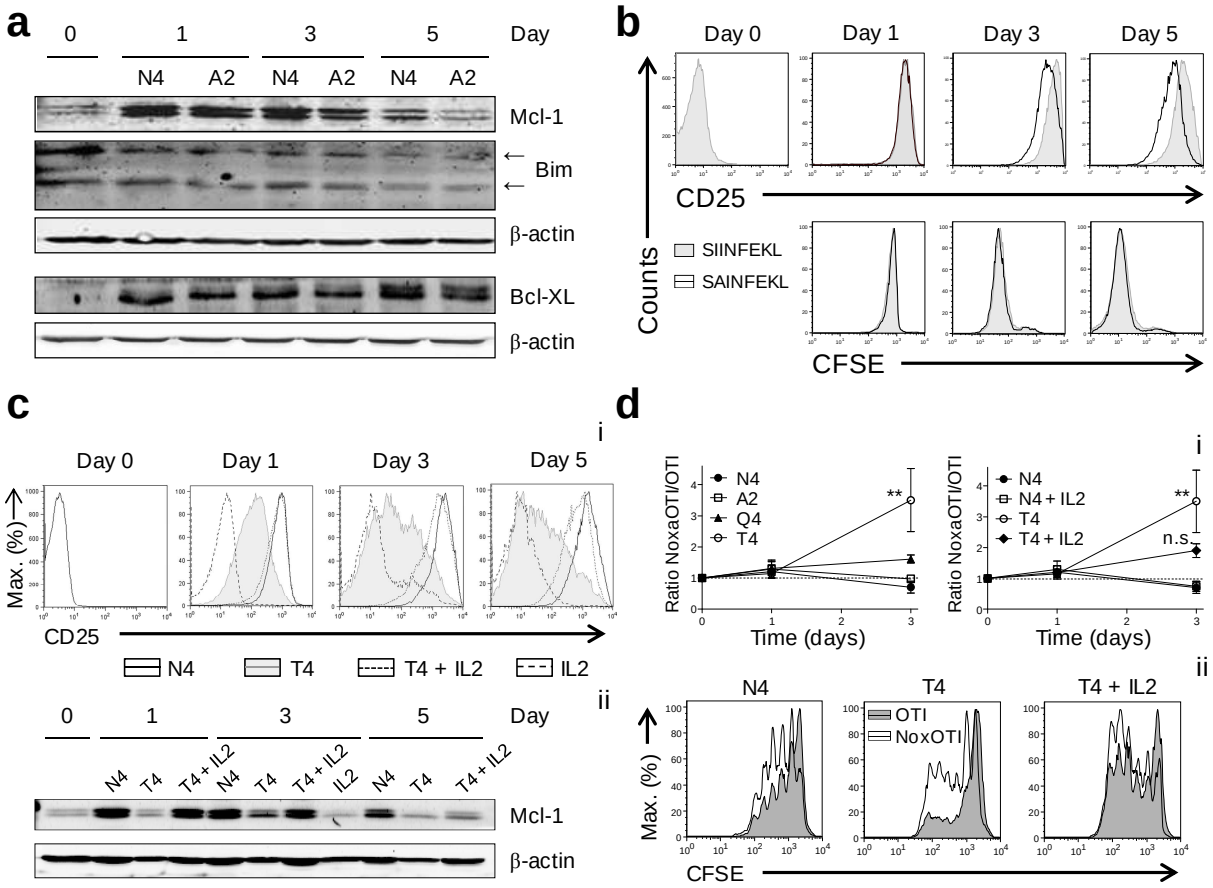

Figure 6. TCR-affinity specifically controls Mcl-1 protein amount via differential IL-2R signalling. a,b Purified splenic OT-1 transgenic T cells were stimulated with 10 ng/ml high affinity SIINFEKL (N4) or low affinity SAINFEKL (A2) peptides as indicated. (**a**) Immunoblot for apoptotic molecules on designated days for N4 or A2 stimulation. Shown is one of six independent experiments with similar results. (**b**) Representative histograms for cells labelled with CFSE and stained with anti-CD25. Shown is one of six independent experiments. **c,** Purified splenic OT-1 transgenic T cells were stimulated with 10 ng/ml IL-2, with 0.1 ng/ml high-affinity SIINFEKL (N4), or low affinity SIITFEKL (T4) peptides or with a combination, as indicated. (**i**) Representative plots of CD25 expression, (**ii**) Mcl-1 expression as determined by western blot. **d,** Purified OT-I or NoxOTI cells were DDAO-labelled before being mixed in a 1:1 ratio. Subsequently these mixed cultures were CFSE labelled and stimulated with altered peptide ligands in the absence or presence of exogenous IL-2. (**i**) NoxOTI/OTI ratio was determined within the AnnexinV$^-$-PI$^-$ population. Stars indicate significant differences compared to N4 stimulated cells. n.s. = not significant. Shown are the combined results of three independent experiments, using two mice of each genotype per experiment (n=6). Error bars indicate s.e.m. (**ii**) Representative CFSE plots show primarily differences within the divided population. See also Figure S5.

Based on the previous data, we hypothesized that in NoxOTI cells Mcl-1 would remain higher after low-affinity TCR stimulation and that this would provide a survival advantage over OT-I cells. Indeed, NoxOTI cells displayed increased amount of Mcl-1 compared to OTI cells after T4 peptide stimulation (**figure S5d,e**). To test survival under competitive conditions, CD8$^+$ T cells were purified from OT-I and NoxOTI mice, mixed in a 1:1 ratio, labeled with carboxyfluorescein diacetate succinimidyl ester (CFSE) and stimulated with OVA peptides of decreasing affinity. The ratio of NoxOTI versus OTI cells was followed over time within the viable (AnnexinV$^-$-PI$^-$) population. Fluorescent labeling was used to distinguish between the two populations (see Methods), which was possible up to three days after stimulation (**Figure S5f**). Noxa ablation provided no advantage for cells

stimulated with N4 peptides, but when peptides of reduced affinity were used, NoxOTI cells survived better, most prominently within the dividing fraction (**Figure 6d**). Moreover, when exogenous IL-2 was added, this survival advantage was abolished due to enhanced survival of dividing OT-I cells. Together, these data indicate that TCR affinity mediates activated T cell survival via differential regulation of IL-2R signaling and indirect modulation of the Noxa-Mcl-1 axis.

Discussion

Based on our data we propose that apoptosis plays an integral role in the formation of effector populations by setting boundaries for expansion during the initial phase after T cell activation. On a molecular level, our primary findings are that pro-apoptotic Noxa is transcriptionally upregulated after a delay upon TCR triggering, and that Mcl-1 is rapidly stabilized on a protein level in a TCR affinity dependent fashion, involving an IL-2-IL-2R signaling loop. On a physiological level, we linked these molecular findings to the formation of high-affinity effector cells upon immune activation by elimination of subdominant clones of low affinity.

Mcl-1 protein is subject to complex regulation by phosphorylation, and binding of Noxa has also been directly implicated in mediating its stability (30,31). In addition, binding of Noxa has been shown to result in competition with Bim for binding places on Mcl-1 (8). Importantly, this latter mechanism may also hold for A1, the other binding partner of Noxa (9), which is also induced upon TCR triggering. Enhanced expression of Noxa would displace Bim, and free Bim is then able to antagonize other pro-survival molecules such as Bcl-XL, or may directly bind Bax to induce apoptosis. The dynamic balance between Noxa, Bim and Mcl-1 may thus set a threshold for survival of high affinity clones in the competitive niche occupied by multiple expanding T cell clones. Lowering of this threshold via ablation of Noxa directly affects the size and quality of effector T cell responses *in vivo*. Activation of T cells thus appears to induce a molecular process that protects cells from apoptosis in the initial stages by upregulation of pro-survival Bcl-2 molecules, but later on sensitizes them to pro-apoptotic stimuli via induction of Noxa.

A prominent candidate for such a stimulus is deprivation of the cytokine IL-2, a member of the γ_c-cytokines linked both to proliferation and survival via the Jak-Stat, MAPK and PI3K signaling pathways (45). Mcl-1, as well as its antagonists Bim and Noxa, have been associated with apoptosis as a result of γ_c-cytokine deprivation (22,44,46). Experiments using growth factor dependent cell lines show that under limiting cytokine concentrations phosphatidylinositol-3-kinase activity is reduced, which leads to glycogen synthase kinase 3 beta-dependent Mcl-1 phosphorylation, ultimately resulting in its proteasomal degradation (28,47). In $CD8^+$ T-cells, Mcl-1 levels are especially sensitive to deprivation of IL-2 (22). Moreover, a recent report showed that TCR triggering with reduced affinity does not affect early replication of OT-1 cells *in vivo* (1), but leads to reduced expression of the receptors for IL-2 and the chemokine receptor CCR7. Our study agrees well with those findings and provides a new link, apart from proliferative differences, between low affinity triggering and reduced expansion. We propose that in a normal setting, low affinity clones will exit the lymph node supposedly as a result of reduced CCR7 expression, and in the periphery through lack of IL-2 signaling undergo apoptosis via the Noxa-Bim-Mcl-1 axis. An essential

component of this scheme is competition between many highly similar T cell clones present in equal amounts in the naïve pool (48). Of note, this competitive aspect is lacking in transgenic models we and others used with a single or a limited set of TCRs (1,2), where the variation in affinity is instead modeled by applying distinct antigenic peptides. Still, the molecular pathways involved can be expected to be similar, and point to a controlling role of IL-2 signaling following low affinity TCR triggers.

Interestingly, two recent papers describe differences in IL-2R signaling strength as a determining factor for the formation of memory or effector T cells by differential regulation of key transcription factors (49,50). In these studies high-affinity TCR triggering was used and differences in CD25 expression occurred several days after activation. Since we found that differences in TCR ligation strength influence CD25 levels rapidly after activation, this appears to be a different mechanism, regulated primarily on a protein level, which precedes the choice via transcription factors of memory or effector cell formation.

In summary, TCR affinity controls the amount of Mcl-1 via IL-2 signaling, and Noxa functions to augment the threshold for survival of activated T cells. Although on a single cell level this has a binary outcome (alive or dead), on a population level it will prevent the persistence of less useful clones that compete with high-affinity clones for limited resources during the expansion phase of activated T cells. Thus, unhindered proliferation and survival of the 'fittest' (i.e. those with the best 'fit' on their MHC-peptide ligand) clones is safeguarded via a Darwinistic selection process

Studies into the role of Bcl-2 proteins in acute infections have focused mostly on the contraction of effector cell populations after clearance of the pathogen (15,51). A strong inducer of apoptosis like Bim is expressed in all T cell subsets from the double positive thymocyte subset onwards. Bim-deficient mice therefore show a profound phenotype during both homeostasis and contraction. Noxa is expressed at very low levels in naïve T cells, but is strongly induced upon activation of these cells, hence our observation that this pro-apoptotic molecule only plays a role during this phase of T cell biology. Considering this notion, it might therefore be predicted that deficiency of Bim, which remains expressed after T cell activation, will also result in increased diversity within the antigen-specific population upon acute infection. A complicating factor in the analysis of these mice is their reduced thymic selection, which results in a naïve compartment of already increased diversity(2,38). It has to be noted that it cannot be formally excluded that Noxa-deficient mice on a clonal level have a naïve compartment of increased diversity compared to wild type mice. However, normal thymic cell numbers and phenotypic composition in Noxa deficient animals, lack of Noxa expression in double positive thymocyte subsets, lack of a survival advantage for anti-CD3 stimulated Noxa deficient DP thymocytes, a normal TCR Vβ usage of their peripheral T cells and a lack of auto-immunity in aged Noxa-deficient mice indicate that this is unlikely. Lastly, the effects of Noxa ablation were maintained in TCR transgenic OT-I mice, again arguing that they occur after thymic selection.

The formation of specific effector cell responses against pathogens must be broad, in the sense that many epitopes are recognized to generate an optimal response, as well as specific to ensure that only a response against relevant epitopes is formed. We argue that these conditions require that on a *per epitope* basis only high-affinity cells are allowed to survive and mount a response. This aspect adds an additional layer of regulation to the

formation of effector cell responses and may have implications for immuno-compromised patients. An inability to form an effective T cell response might not only result from poor T cell activation, but also from impaired selective pressure. Modern therapeutic techniques, such as in vitro administration of co-stimulatory molecules to boost T cell responses, might therefore be counterproductive without simultaneous attempts to increase specificity of the response. Our preliminary data indicate that Noxa ablation actually induces organ pathology as a result of a specific effector cell accumulation (Wensveen *et al.*, unpublished observations). Our findings therefore have implications for the understanding of viral disease progression, the design of vaccination strategies and antiviral drug development. Finally, based on the depletion of the naïve compartment in aged Noxa-deficient mice, it can be envisaged that also memory formation and/or function is affected by impaired initial T cell selection.

In conclusion, deficiency of pro-apoptotic Noxa leads to persistence of suboptimal T cell clones, causing the generation of a less efficient effector population in acute responses and resulting in effector memory cell accumulation in aged mice. These findings show that apoptosis during the expansion phase is crucial for shaping adaptive immune responses, with implications for acute and chronic infections, as well as ageing of the immune system.

Acknowledgements

We wish to thank Andreas Strasser for providing the Noxa-deficient mice, Marco Breuer and Tatjana Westphal (Netherlands Cancer Institute) for the *p53*$^{-/-}$ tissues, Dietmar Zehn and Michael Bevan (HHMI, Seatle, USA) for providing the Listeria strains and the staff of the AMC animal facility for excellent animal care. We are grateful to Berend Hooibrink, Sven Koch, Ester Remmerswaal, René Spijker, Ronald Van Olffen and to Koen van der Sluijs for technical assistance, and thank Sandrine Florquin for the pathological analysis of the tissues. Koen Oosterhuis helped with the DNA tattooing, and Louis Boon generously provided antibodies. We would like to thank Paul Klarenbeek and Martijn Nolte for encouraging discussions and critical reading of the manuscript. This study was partly funded by an NWO VICI grant to RvL.

Materials and Methods

Mice

C57BL/6 (B6), OT-1 and B6 Ly5.1^{+} JAX® mice were purchased from Charles River and kept as breeding colonies in our local animal facility. Only these mice, which were kept under identical conditions as our transgenic and gene ablated mice, were used as WT controls in our experiments. Noxa-deficient mice were a kind gift from Dr. A. Strasser (WEHI, Melbourne) and provided by Dr. M. Serrano (CNIO, Madrid). Noxa5.1 mice were generated by crossing Noxa-deficient mice with B6 Ly5.1^{+} mice from our in house colony. NoxOTI mice were generated by crossing Noxa-deficient mice with B6 OT-1 mice from our in house colony. *p53*$^{-/-}$ tissues were a gift from Dr. M. Breuer (NKI, Amsterdam). TNFRFS7-deficient, B cel specific CD70^{TG} and TNFRFS7-deficient^{-}CD70^{TG} mice were generated as previously described (Hendriks et al. Nat. Immunol. 2000, Arens et al. *Immunity* 2001, Van Gisbergen et al. *J. Immunol.* 2009). Mice were used at 6-12 weeks of age, unless stated otherwise, age- and

sex-matched within experiments and were handled in accordance with institutional and national guidelines. All experiments were performed using protocols approved by our institutional ethical committee.Apart from the *p53*$^{-/-}$ mice (BALB/c), all mice were either generated in B6 mice or backcrossed at least ten times on this background.

Flow Cytometry

Single-cell suspensions were obtained by mincing the specified organs through 40 □m cell strainers (Becton Dickinson). Erythrocytes were lysed with an ammonium chloride solution (155 mM NH4Cl, 10 mM $KHCO_3$, and 1 mM EDTA) and cells were subsequently counted using an automated cell counter (SCHÄRFE SYSTEM). Cells (5 x 10^5- 5 x 10^6) were collected in staining buffer (PBS with 0.5% bovine serum albumin (Sigma)) and stained for 30 min at 4˚C with antibodies in the presence of anti-CD16/CD32 (clone 2.4G2, anti-mouse FcγRII-RIII (a kind gift of Louis Boon, Bioceros, Utrecht, the Netherlands). For a list of the monoclonal antibodies used see Supplementary Table S1. Conjugated D^bNP366 and K^bOVA tetramers were obtained from Sanquin (http://www.sanquin.nl). FACS™ experiments were performed on a FACSCalibur™ or FACSCanto™ (Becton Dickinson) and analysed with FlowJo™ software (TriStar). Cell viability, was assessed by staining with FITC conjugated AnnexinV (BD bBiosciences) followed by adding 100 nM To-Pro-3 (Molecular Probes) shortly before measurement. Naïve ($CD3^+CD4^-CD8^+CD44^-CD62L^+D^bNP366^-$) and NP366 specific ($CD3^+CD4^-CD8^+D^bNP366^+$) CTLs were sorted to >99% purity with a FACSAria™ (Becton Dickinson).

Cell culture

Spleen derived T cells were purified to > 95% purity by positive or negative selection using the MACS cell separation system (Myltenyi). $CD8^+$ T cells were positively selected with anti-CD8 microbeads (Myltenyi). Cells were stimulated in RPMI medium with 10% fetal calf serum FCS with solid phase anti-CD3 (145-2C11) alone, in combination with soluble anti-CD28 (37.51), (both a kind gift of Louis Boon). DNA-damage mediated apoptosis was induced by 2.5 Gy γ-irradiation, using a ^{137}CS-source. Purified OT-I T cells were stimulated in vitro with 0.1, 1 or 10 ng/ml SIINFEKL (N4), SAINFEKL (A2), SIITFEKL (T4) or SIIQFEKL (Q4 peptides. Where indicated, 10 ng/ml IL-2 (R&D Research) was added. Cell division was analyzed by carboxyfluorescein diacetate succinimidyl ester (CFSE, Molecular Probes) dilution. In mixed colonies, OT-I or NoxOTI cells were labelled with 7-hydroxy-9H(I,3-dichloro-9,9-dimethylacridin-2-one succinimidyl ester (DDAO-SE, Molecular Probes) to distinguish between populations. Activation status of T cell subsets was analyzed by anti-CD69 and anti-CD25 or CD44 and CD62L staining.

RT-MLPA analysis

Total RNA for Reverse Transcriptase Multiplex Ligation-dependent Probe Amplification (RT-MLPA) was extracted using the trizol isolation method (Invitrogen). mRNA amounts were analyzed with the Apoptosis Mouse RT-MLPA kit RM002 (MRC-Holland, http://www.mlpa.com) according to the manufacturer's instructions. Samples were run through a Genescan and analyzed with GeneMapper (Applied Biosystems GmbH;

http://www.appliedbiosystems.com) and subsequently with Excell software (Microsoft), as described previously (Eldering et al., 2003, Alves et al., 2006).

Influenza infection, DNA-Tattooing, SEB, adoptive transfer and Listeria infection

Influenza A virus of the A/PR8/34 strain (H1N1) was generated in LLC-MK2 cells and $TCID_{50}$ was determined in wild type B6 mice. Mice were infected intranasally with 10 x $TCID_{50}$. Virus titers were determined by quantitative polmerase chain reaction (qPCR)as described (52), using the primers: 5′-GGACTGCAGCGTAGACGCTT-3′ (forward); 5′-CATCCTGTTGTATATGA GGCCCAT-3′ (reverse), 5′-CTCAGTTATTCTGCTGGTGCACTTGCC-3′ (5′-FAM labeled probe). DNA-Tattooing was performed basically as described(37). Briefly, 30 μg of d1TTFC-SIINFEKL DNA-constructs were applied on the skin of the hind leg after hair removal using depilatory cream (VEET®, ReckittBenckiser), and administered using Permanment Make Up® tattoo machine (MT Derm GmbH, Berlin, Germany). Tattooing was performed with a disposable 9 needle bar oscilating at 100HZ for 30 sec at a depth of 1 mm, the procedure was repeated twice with two day intervals. Staphylococcal enterotoxin B (Sigma) was dissolved in PBS and 20μg per mouse was injected intraperitonal. For adoptive transfer to study polyclonal responses, total T cells of WT and Noxa-deficient mice (both $Ly5.1^{+}$) were isolated from spleens by positive selection for $CD4^{+}$ and $CD8^{+}$ T cells using the MACS cell separation system (Myltenyi). Cells were injected intravenous in TNFRFS7-deficient and TNFRFS7-deficient-$^{-}CD70^{TG}$ mice. After 24hrs transfer efficiency was determined by $FACS^{TM}$. For adoptive transfer to study monoclonal responses, $CD8^{+}$ T cells of OT-I and NoxOTI mice (both $Ly5.2^{-+}$) were isolated from spleens by positive selection for $CD4^{+}$ and $CD8^{+}$ using the MACS cell separation system (Myltenyi). 5000 cells per mouse were injected intravenously in wild type ($Ly5.1^{+}$) recipients. Infection with a Listeria monocytogenes strain expressing the SIINFEKL (N4) or SIITFEKL (T4) sequence (Zehn et al., 2009) occurred intravenously at 2500 colony forming units (CFU), one day after transfer of cells.

Immunoprecipitation, immunoblot, RT-PCR and histochemistry

For immunoprecipitation cells were lysed in a 1% Triton X100-containing lysis buffer at the indicated time points after anti-CD3 and anti-CD28 stimulation. Cell lysates were precleared with normal rabbit serum coupled to protein A-sepharose (Sigma) followed by an immunoprecipitation with Mcl-1 antibody coupled to protein A-sepharose. Beads were pelleted, washed 6 times and boiled in sample buffer for Western blot analysis, using the Bio-Rad mini-PROTEAN electrophoresis system as described (24) with primary antibodies against β-Actin (Santa Cruz Biotechnology), Bim (Stressgen), Bcl-XL (Transduction Laboratories) and Mcl-1 (Rockland). Staining was visualised using IRDye 680 or 800 labeled secondary antibodies and an Odyssey Imager (Li-Cor). Quantification of signal was performed using Odyssey 3.0 software. Total RNA was extracted using the Trizol isolation method (Invitrogen) and cDNA was generated using oligodeoxythymidine (oligo dT) and Superscript II Reverse Transcriptase (Invitrogen). Noxa transcripts were amplified by polymerase chain reaction (PCR) using Noxa sense and antisense primers (5'-CTCTCGAGCCCGGGAGAAAGGCGC-3' and 5'-GGGAATTCTCAGGTTACTAAA TTGAAGAGCT-3') and 18S was used as a loading control (5'-TCAAGAACGAAAGT

CGGAGG-3' and 5'-GGACATCTAAGGGCATCACA-3'). For histochemistry, formaldehyde fixed tissues were imbedded in parafin. For histochemcal analysis, sections were stained with haematoxylin and eosin.

Intracellular cytokine staining
To determine direct ex vivo cytokine production, splenocytes were plated at 1 x 10^6 cells/well in a 96-well round-bottom plate and stimulated with 10 ng/ml phorbol 12-myristate 13-acetate (PMA) and 1 uM ionomycin (Sigma) or with increasing concentrations of peptide (ASNENMDAM, or SIINFEKL; Genscript, http://www.genscript.com) for 6hrs at 37°C. During the final 4 hours, 1 μg/ml of the protein-secretion inhibitor Brefeldin A (Sigma) was added. Thereafter, cells were washed and stained with anti-CD4 or anti-CD8, followed by fixation and permeabilization (Becton Dickinson). Cells were then incubated for 30 min with fluorescently labelled antibodies against IFNγ, TNFα, IL-2, IL-10 or IL-17, thoroughly washed and analyzed by flow cytometry.

PCR analysis of TCR clones.
Cells were sorted on day 9 and 10 after infection and cDNA was generated from mRNA after extraction using the Trizol isolation method. TCR Vβ-Cβ elements were amplified by PCR, using the Vβ5.2 primer (5'-AAGGTGGAGAGAGACAAAGGATTC-3') or the Vβ8.3 primer (5'-TGCTGGCAACCTTCGAATAGGA-3') in combination with a FAM-labeled Cβ1 primer (5'-CTTGGGTGGAGTCACATTTCTC-3'). Products were run through a Genescan and analyzed with GeneMapper (ABI) for spectratyping. Simultaneously, the PCR product was cloned in pGEM-T (Promega) and colonies positive for the Vβ5.2 or 8.3 gene element were sequenced. Sequence reactions were performed using the Big Dye Terminator kit (Applied Biosystems) and sequence analysis was executed by an in-house facility. The sequences were analyzed online, using the International ImMunoGeneTics information system (IMGT) (http://imgt.cines.fr). Clones containing two or more basepair differences with all other clones were defined as unique.

Statistical analysis Statistical analysis of the data was performed using the unpaired Student's *t*-test, Wilcoxon rank-sum test or one-way ANOVA test where applicable. Asterisks denote significant differences (* $p<0.05$, ** $p<0.005$, *** $p<0.0005$).

Reference List

1. Zehn, D., S. Y. Lee, and M. J. Bevan. 2009. Complete but curtailed T-cell response to very low-affinity antigen. *Nature* 458: 211-214.
2. Malherbe, L., C. Hausl, L. Teyton, and M. G. Heyzer-Williams. 2004. Clonal selection of helper T cells is determined by an affinity threshold with no further skewing of TCR binding properties. *Immunity.* 21: 669-679.
3. Green, D. R., and G. I. Evan. 2002. A matter of life and death. *Cancer Cell* 1: 19-30.
4. Youle, R. J., and A. Strasser. 2008. The BCL-2 protein family: opposing activities that mediate cell death. *Nat. Rev. Mol. Cell Biol.* 9: 47-59.
5. Merino, D., M. Giam, P. D. Hughes, O. M. Siggs, K. Heger, L. A. O'Reilly, J. M. Adams, A. Strasser, E. F. Lee, W. D. Fairlie, and P. Bouillet. 2009. The role of BH3-only protein Bim extends beyond inhibiting Bcl-2-like prosurvival proteins. *J. Cell Biol.* 186: 355-362.
6. Kim, H., H. C. Tu, D. Ren, O. Takeuchi, J. R. Jeffers, G. P. Zambetti, J. J. Hsieh, and E. H. Cheng. 2009. Stepwise activation of BAX and BAK by tBID, BIM, and PUMA initiates mitochondrial apoptosis. *Mol. Cell* 36: 487-499.
7. Willis, S. N., J. I. Fletcher, T. Kaufmann, M. F. van Delft, L. Chen, P. E. Czabotar, H. Ierino, E. F. Lee, W. D. Fairlie, P. Bouillet, A. Strasser, R. M. Kluck, J. M. Adams, and D. C. Huang. 2007. Apoptosis initiated when BH3 ligands engage multiple Bcl-2 homologs, not Bax or Bak. *Science* 315: 856-859.
8. Kim, H., M. Rafiuddin-Shah, H. C. Tu, J. R. Jeffers, G. P. Zambetti, J. J. Hsieh, and E. H. Cheng. 2006. Hierarchical regulation of mitochondrion-dependent apoptosis by BCL-2 subfamilies. *Nat. Cell Biol.* 8: 1348-1358.
9. Chen, L., S. N. Willis, A. Wei, B. J. Smith, J. I. Fletcher, M. G. Hinds, P. M. Colman, C. L. Day, J. M. Adams, and D. C. Huang. 2005. Differential targeting of prosurvival Bcl-2 proteins by their BH3-only ligands allows complementary apoptotic function. *Mol. Cell* 17: 393-403.
10. Bouillet, P., D. Metcalf, D. C. Huang, D. M. Tarlinton, T. W. Kay, F. Kontgen, J. M. Adams, and A. Strasser. 1999. Proapoptotic Bcl-2 relative Bim required for certain apoptotic responses, leukocyte homeostasis, and to preclude autoimmunity. *Science* 286: 1735-1738.
11. Jeffers, J. R., E. Parganas, Y. Lee, C. Yang, J. Wang, J. Brennan, K. H. MacLean, J. Han, T. Chittenden, J. N. Ihle, P. J. McKinnon, J. L. Cleveland, and G. P. Zambetti. 2003. Puma is an essential mediator of p53-dependent and -independent apoptotic pathways. *Cancer Cell* 4: 321-328.
12. Yin, X. M., K. Wang, A. Gross, Y. Zhao, S. Zinkel, B. Klocke, K. A. Roth, and S. J. Korsmeyer. 1999. Bid-deficient mice are resistant to Fas-induced hepatocellular apoptosis. *Nature* 400: 886-891.
13. Kaufmann, T., P. J. Jost, M. Pellegrini, H. Puthalakath, R. Gugasyan, S. Gerondakis, E. Cretney, M. J. Smyth, J. Silke, R. Hakem, P. Bouillet, T. W. Mak, V. M. Dixit, and A. Strasser. 2009. Fatal hepatitis mediated by tumor necrosis factor TNFalpha requires caspase-8 and involves the BH3-only proteins Bid and Bim. *Immunity.* 30: 56-66.
14. Erlacher, M., V. Labi, C. Manzl, G. Bock, A. Tzankov, G. Hacker, E. Michalak, A. Strasser, and A. Villunger. 2006. Puma cooperates with Bim, the rate-limiting BH3-only protein in cell death during lymphocyte development, in apoptosis induction. *J. Exp. Med.* 203: 2939-2951.
15. Fischer, S. F., G. T. Belz, and A. Strasser. 2008. BH3-only protein Puma contributes to death of antigen-specific T cells during shutdown of an immune response to acute viral infection. *Proc. Natl. Acad. Sci. U. S. A* 105: 3035-3040.
16. Opferman, J. T., and S. J. Korsmeyer. 2003. Apoptosis in the development and maintenance of the immune system. *Nat. Immunol.* 4: 410-415.
17. Villunger, A., E. M. Michalak, L. Coultas, F. Mullauer, G. Bock, M. J. Ausserlechner, J. M. Adams, and A. Strasser. 2003. p53- and drug-induced apoptotic responses mediated by BH3-only proteins puma and noxa. *Science* 302: 1036-1038.
18. Coultas, L., P. Bouillet, E. G. Stanley, T. C. Brodnicki, J. M. Adams, and A. Strasser. 2004. Proapoptotic BH3-only Bcl-2 family member Bik/Blk/Nbk is expressed in hemopoietic and endothelial cells but is redundant for their programmed death. *Mol. Cell Biol.* 24: 1570-1581.

19. Datta, S. R., A. M. Ranger, M. Z. Lin, J. F. Sturgill, Y. C. Ma, C. W. Cowan, P. Dikkes, S. J. Korsmeyer, and M. E. Greenberg. 2002. Survival factor-mediated BAD phosphorylation raises the mitochondrial threshold for apoptosis. *Dev. Cell* 3: 631-643.
20. Labi, V., M. Erlacher, S. Kiessling, C. Manzl, A. Frenzel, L. O'Reilly, A. Strasser, and A. Villunger. 2008. Loss of the BH3-only protein Bmf impairs B cell homeostasis and accelerates gamma irradiation-induced thymic lymphoma development. *J. Exp. Med.* 205: 641-655.
21. Ranger, A. M., J. Zha, H. Harada, S. R. Datta, N. N. Danial, A. P. Gilmore, J. L. Kutok, M. M. Le Beau, M. E. Greenberg, and S. J. Korsmeyer. 2003. Bad-deficient mice develop diffuse large B cell lymphoma. *Proc. Natl. Acad. Sci. U. S. A* 100: 9324-9329.
22. Bosque, A., I. Marzo, J. Naval, and A. Anel. 2007. Apoptosis by IL-2 deprivation in human CD8+ T cell blasts predominates over death receptor ligation, requires Bim expression and is associated with Mcl-1 loss. *Mol. Immunol.* 44: 1446-1453.
23. Oda, E., R. Ohki, H. Murasawa, J. Nemoto, T. Shibue, T. Yamashita, T. Tokino, T. Taniguchi, and N. Tanaka. 2000. Noxa, a BH3-only member of the Bcl-2 family and candidate mediator of p53-induced apoptosis. *Science* 288: 1053-1058.
24. Alves, N. L., I. A. Derks, E. Berk, R. Spijker, R. A. van Lier, and E. Eldering. 2006. The Noxa/Mcl-1 axis regulates susceptibility to apoptosis under glucose limitation in dividing T cells. *Immunity* 24: 703-716.
25. Alves, N. L., R. A. van Lier, and E. Eldering. 2007. Withdrawal symptoms on display: Bcl-2 members under investigation. *Trends Immunol.* 28: 26-32.
26. Eldering, E., C. A. Spek, H. L. Aberson, A. Grummels, I. A. Derks, A. F. de Vos, C. J. McElgunn, and J. P. Schouten. 2003. Expression profiling via novel multiplex assay allows rapid assessment of gene regulation in defined signalling pathways. *Nucleic Acids Res.* 31: e153.
27. Lee, H. W., S. J. Park, B. K. Choi, H. H. Kim, K. O. Nam, and B. S. Kwon. 2002. 4-1BB promotes the survival of CD8+ T lymphocytes by increasing expression of Bcl-xL and Bfl-1. *J. Immunol.* 169: 4882-4888.
28. Maurer, U., C. Charvet, A. S. Wagman, E. Dejardin, and D. R. Green. 2006. Glycogen synthase kinase-3 regulates mitochondrial outer membrane permeabilization and apoptosis by destabilization of MCL-1. *Mol. Cell* 21: 749-760.
29. Zhong, Q., W. Gao, F. Du, and X. Wang. 2005. Mule/ARF-BP1, a BH3-only E3 ubiquitin ligase, catalyzes the polyubiquitination of Mcl-1 and regulates apoptosis. *Cell* 121: 1085-1095.
30. Czabotar, P. E., E. F. Lee, M. F. van Delft, C. L. Day, B. J. Smith, D. C. Huang, W. D. Fairlie, M. G. Hinds, and P. M. Colman. 2007. Structural insights into the degradation of Mcl-1 induced by BH3 domains. *Proc. Natl. Acad. Sci. U. S. A* 104: 6217-6222.
31. Dzhagalov, I., A. Dunkle, and Y. W. He. 2008. The anti-apoptotic Bcl-2 family member Mcl-1 promotes T lymphocyte survival at multiple stages. *J. Immunol.* 181: 521-528.
32. Lerner, A., T. Yamada, and R. A. Miller. 1989. Pgp-1hi T lymphocytes accumulate with age in mice and respond poorly to concanavalin A. *Eur. J. Immunol.* 19: 977-982.
33. Kedzierska, K., E. B. Day, J. Pi, S. B. Heard, P. C. Doherty, S. J. Turner, and S. Perlman. 2006. Quantification of repertoire diversity of influenza-specific epitopes with predominant public or private TCR usage. *J. Immunol.* 177: 6705-6712.
34. Venturi, V., K. Kedzierska, S. J. Turner, P. C. Doherty, and M. P. Davenport. 2007. Methods for comparing the diversity of samples of the T cell receptor repertoire. *J. Immunol. Methods* 321: 182-195.
35. Zhong, W., and E. L. Reinherz. 2004. In vivo selection of a TCR Vbeta repertoire directed against an immunodominant influenza virus CTL epitope. *Int. Immunol.* 16: 1549-1559.
36. Klenerman, P., and A. Hill. 2005. T cells and viral persistence: lessons from diverse infections. *Nat. Immunol.* 6: 873-879.
37. Bins, A. D., A. Jorritsma, M. C. Wolkers, C. F. Hung, T. C. Wu, T. N. Schumacher, and J. B. Haanen. 2005. A rapid and potent DNA vaccination strategy defined by in vivo monitoring of antigen expression. *Nat. Med.* 11: 899-904.
38. Bouillet, P., J. F. Purton, D. I. Godfrey, L. C. Zhang, L. Coultas, H. Puthalakath, M. Pellegrini, S. Cory, J. M. Adams, and A. Strasser. 2002. BH3-only Bcl-2 family member Bim is required for apoptosis of autoreactive thymocytes. *Nature* 415: 922-926.

39. White, J., A. Herman, A. M. Pullen, R. Kubo, J. W. Kappler, and P. Marrack. 1989. The V beta-specific superantigen staphylococcal enterotoxin B: stimulation of mature T cells and clonal deletion in neonatal mice. *Cell* 56: 27-35.
40. van Gisbergen, K. P., R. W. van Olffen, B. J. van, K. F. van der Sluijs, R. Arens, M. A. Nolte, and R. A. van Lier. 2009. Protective CD8 T cell memory is impaired during chronic CD70-driven costimulation. *J. Immunol.* 182: 5352-5362.
41. Tesselaar, K., R. Arens, G. M. van Schijndel, P. A. Baars, d. van, V, J. Borst, M. H. van Oers, and R. A. van Lier. 2003. Lethal T cell immunodeficiency induced by chronic costimulation via CD27-CD70 interactions. *Nat. Immunol.* 4: 49-54.
42. Arens, R., K. Tesselaar, P. A. Baars, G. M. van Schijndel, J. Hendriks, S. T. Pals, P. Krimpenfort, J. Borst, M. H. van Oers, and R. A. van Lier. 2001. Constitutive CD27/CD70 interaction induces expansion of effector-type T cells and results in IFNgamma-mediated B cell depletion. *Immunity.* 15: 801-812.
43. Joshi, N. S., W. Cui, A. Chandele, H. K. Lee, D. R. Urso, J. Hagman, L. Gapin, and S. M. Kaech. 2007. Inflammation directs memory precursor and short-lived effector CD8(+) T cell fates via the graded expression of T-bet transcription factor. *Immunity.* 27: 281-295.
44. Huntington, N. D., H. Puthalakath, P. Gunn, E. Naik, E. M. Michalak, M. J. Smyth, H. Tabarias, M. A. gli-Esposti, G. Dewson, S. N. Willis, N. Motoyama, D. C. Huang, S. L. Nutt, D. M. Tarlinton, and A. Strasser. 2007. Interleukin 15-mediated survival of natural killer cells is determined by interactions among Bim, Noxa and Mcl-1. *Nat. Immunol.* 8: 856-863.
45. Benczik, M., and S. L. Gaffen. 2004. The interleukin (IL)-2 family cytokines: survival and proliferation signaling pathways in T lymphocytes. *Immunol. Invest* 33: 109-142.
46. Huntington, N. D., V. Labi, A. Cumano, P. Vieira, A. Strasser, A. Villunger, J. P. Di Santo, and N. L. Alves. 2009. Loss of the pro-apoptotic BH3-only Bcl-2 family member Bim sustains B lymphopoiesis in the absence of IL-7. *Int. Immunol.* 21: 715-725.
47. Morel, C., S. M. Carlson, F. M. White, and R. J. Davis. 2009. Mcl-1 integrates the opposing actions of signaling pathways that mediate survival and apoptosis. *Mol. Cell Biol.* 29: 3845-3852.
48. Nikolich-Zugich, J., M. K. Slifka, and I. Messaoudi. 2004. The many important facets of T-cell repertoire diversity. *Nat. Rev. Immunol.* 4: 123-132.
49. Pipkin, M. E., J. A. Sacks, F. Cruz-Guilloty, M. G. Lichtenheld, M. J. Bevan, and A. Rao. 2010. Interleukin-2 and Inflammation Induce Distinct Transcriptional Programs that Promote the Differentiation of Effector Cytolytic T Cells. *Immunity.* 32: 79-90.
50. Kalia, V., S. Sarkar, S. Subramaniam, W. N. Haining, K. A. Smith, and R. Ahmed. 2010. Prolonged Interleukin-2Ralpha Expression on Virus-Specific CD8(+) T Cells Favors Terminal-Effector Differentiation In Vivo. *Immunity.* 32: 91-103.
51. Pellegrini, M., G. Belz, P. Bouillet, and A. Strasser. 2003. Shutdown of an acute T cell immune response to viral infection is mediated by the proapoptotic Bcl-2 homology 3-only protein Bim. *Proc. Natl. Acad. Sci. U. S. A* 100: 14175-14180.
52. Dessing, M. C., K. F. van der Sluijs, S. Florquin, and P. T. van der. 2007. Monocyte chemoattractant protein 1 contributes to an adequate immune response in influenza pneumonia. *Clin. Immunol.* 125: 328-336.

Supplementary Figures

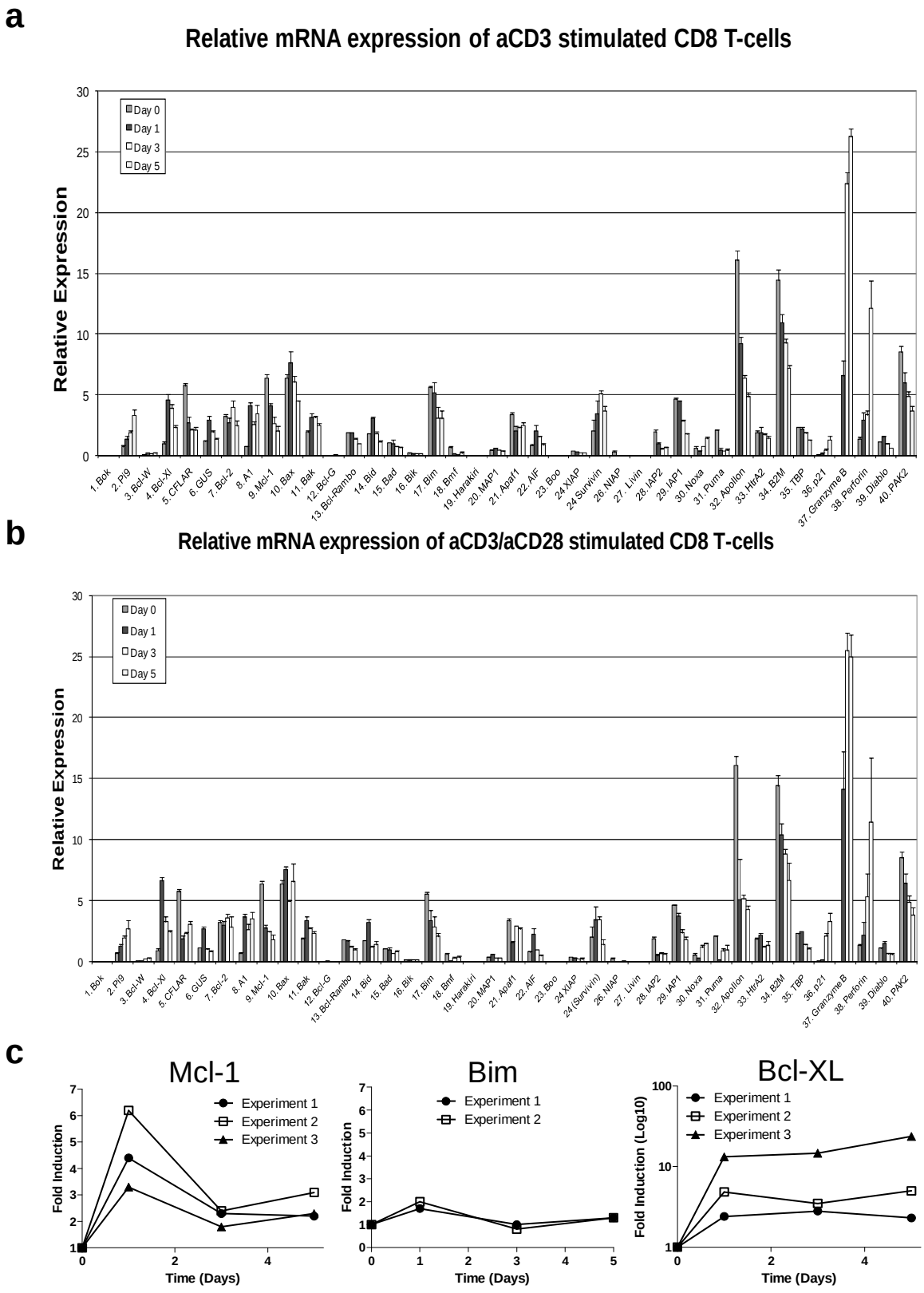

Supplementary Figure S1. Differential apoptotic gene expression in TCR-stimulated T cells Expression profiling of purified CD8 T cells after TCR stimulation by RT-MLPA. **a, b,** purified CD8 T cells were stimulated with (**a**) coated anti-CD3 only, or (**b**) in combination with soluble anti-CD28. (**c**), Quantification of western blot analysis of CD8 T cells after anti-CD3/anti-CD28 stimulation, showing transient Mcl-1 stabilization.

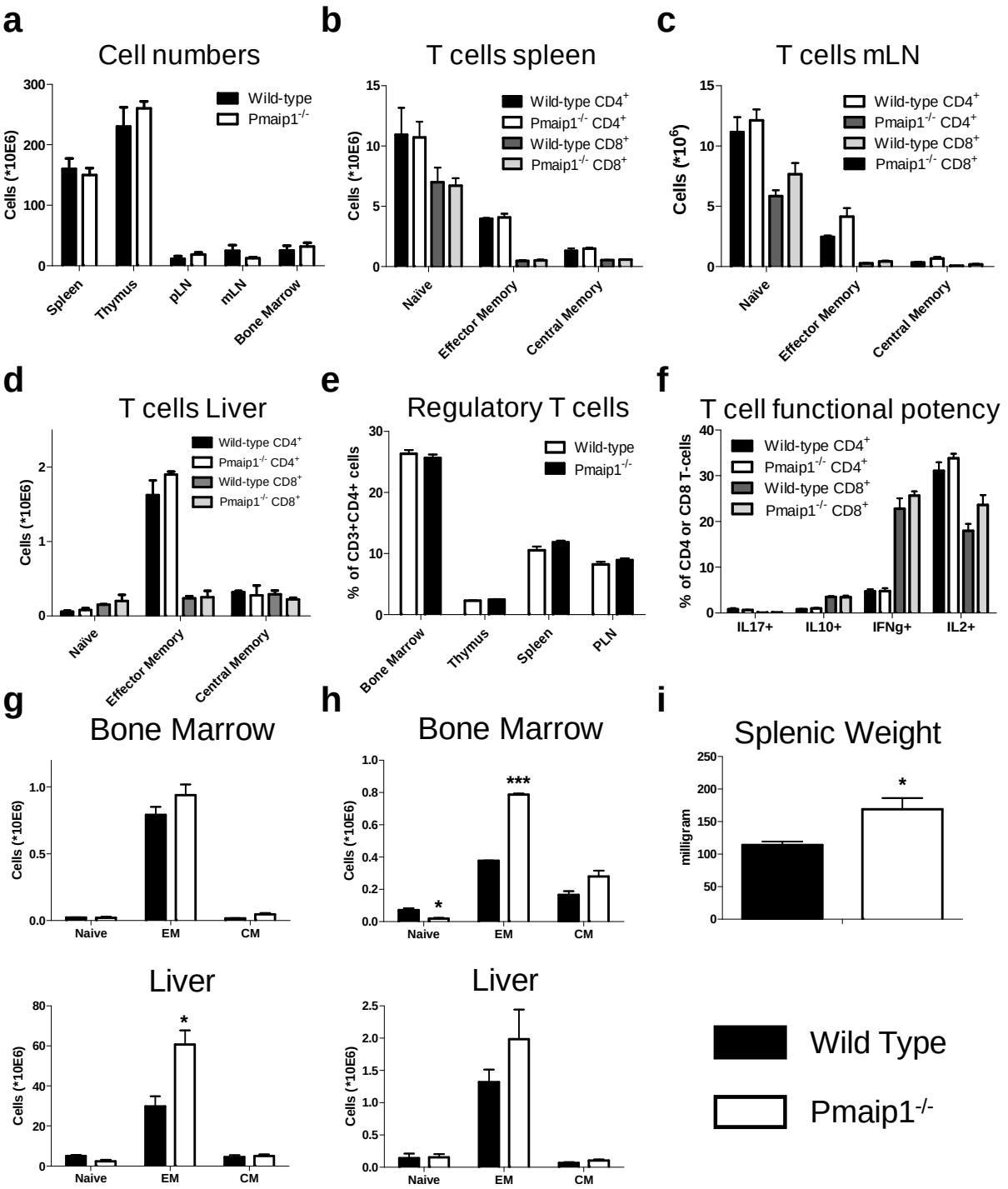

Supplementary Figure S2. Analysis of the peripheral T cell compartment of young and aged Noxa$^{-/-}$ mice under homeostatic conditions a-f Phenotypic analysis of the peripheral T cell compartments of young (8-12wk) wild type and Pmaip1$^{-/-}$ mice. **a**, Absolute number of cells in primary and secondary lymphoid organs, **b-d**, Absolute number of CD4^{+} and CD8^{+} T cell subsets in the (**a**) spleen, (**b**) mesenteric lymph nodes (mLN) and (**c**) Liver based on CD44 and CD62L expression. **e**, Relative number of regulatory T cells in the indicated organs, based on the expression of CD3, CD4, CD25 and FoxP3. **f**, Average production of IL-17, IL-10, IFNγ and IL-2 by CD4^{+} and CD8^{+} T cells, following PMA/Ionomycin stimulation in the presence of Brefeldin A. **g-i**, Wild Type (black bars) and Pmaip1$^{-/-}$ (white bars) mice were analyzed at 18 months of age. **g**, **h** Shown are the absolute numbers of naïve, effector memory (EM) and central memory (CM) cells for (**g**) CD4 and (**h**) CD8 positive T cells in the Bone marrow and liver. **i**, Splenic weight from aged wild type and Noxa$^{-/-}$ mice. Shown are the means ± s.e.m. of two or more experiments using 3 or 4 mice per group per experiment. Values represent means ± s.e.m. (WT n = 3, Pmaip1$^{-/-}$ n = 4), * p<0.05, *** p < 0,0005.

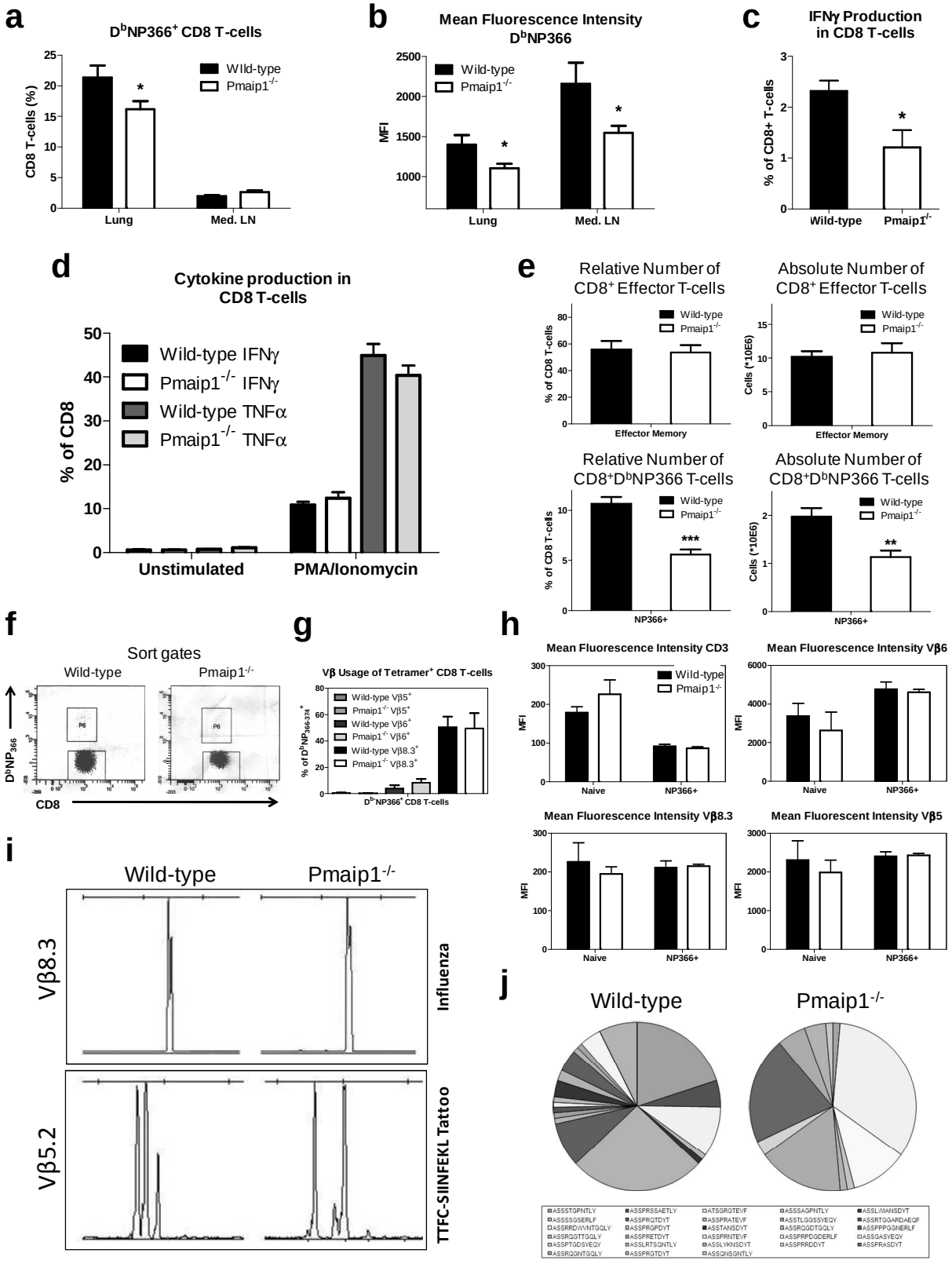

Supplementary Figure S3. Phenotypic and functional analysis of antigen-specific T cells a-i WT and Pmaip1$^{-/-}$ mice were infected with the Influenza virus A/PR8/34. At the peak of the response (day 9-10), organs were isolated and analyzed. **a**, Percentage of D^{b}NP366 positive cells in the lung and medistinal lymph nodes (Med. LN) **b**, MFI of D^{b}NP366 cells in the indicated organs **c**, Percentage of IFNγ producing CD8 T cells after stimulation with 1000ng/ml $NP_{366-374}$ peptide. **d**, IFNγ and TNF

IFNγ producing CD8 T cells after stimulation with 1000ng/ml $NP_{366-374}$ peptide. **d**, IFNγ and TNF production in CD8 T cells incubated in medium only or with PMA/Ionomycin shows that $Pmaip1^{-/-}$ CD8 T cells have no general functional impairment. **e**, Percentage (left) and absolute number (right) of splenic effector memory CD8 T cells (top panels) and D^bNP366^+ CD8 T cells (bottom panels). Shown are values ± s.e.m. (n = 4). Asterisks denote significant differences (* p< 0,005, ** p < 0,0005). **f** Flow cytometry sort gates for virus specific ($CD3^+CD4^-CD8^+D^b$-$NP_{366-374}^+$, P6) cells purified from total splenocytes. **g**, Vβ usage of three different families within the D^b-$NP_{366-374}^+$ CD8 T cell compartment shown for wild type and $Pmaip1^{-/-}$ mice. **h,** Comparison of CD3 and Vβ expression level within the naïve and D^b-$NP_{366-374}^+$ CD8 T cell compartments of wild type (black bars) and $Pmaip1^{-/-}$ (white bars) mice based on the mean fluorescence intensity. Shown are means ± s.e.m. (n = 4).i,j WT and $Pmaip1^{-/-}$ mice were immunized with TTFC-SIINFEKL via DNA-tattoo. At the peak of the response, organs were isolated and analyzed. **i**, spectratype analysis of D^b-NP366 specific T cells after Influenza infection and of K^b-SIINFEKL (K^bOVA) specific T cells after TTFC-SIINFEKL Tattoo shows a more restricted CDR3 length distribution after influenza infection. **j**, Cumulative clonal composition of the $Vβ5.2^+K^bOVA^+$ CD8 T cell population in WT and $Noxa^{-/-}$ mice. Given is the relative contribution of each clone to the total $Vβ5.2^+K^bOVA^+$ population analysed (WT n = 73, $Noxa^{-/-}$ n = 72 clones, amino acid sequence of CDR3 regions is indicated.

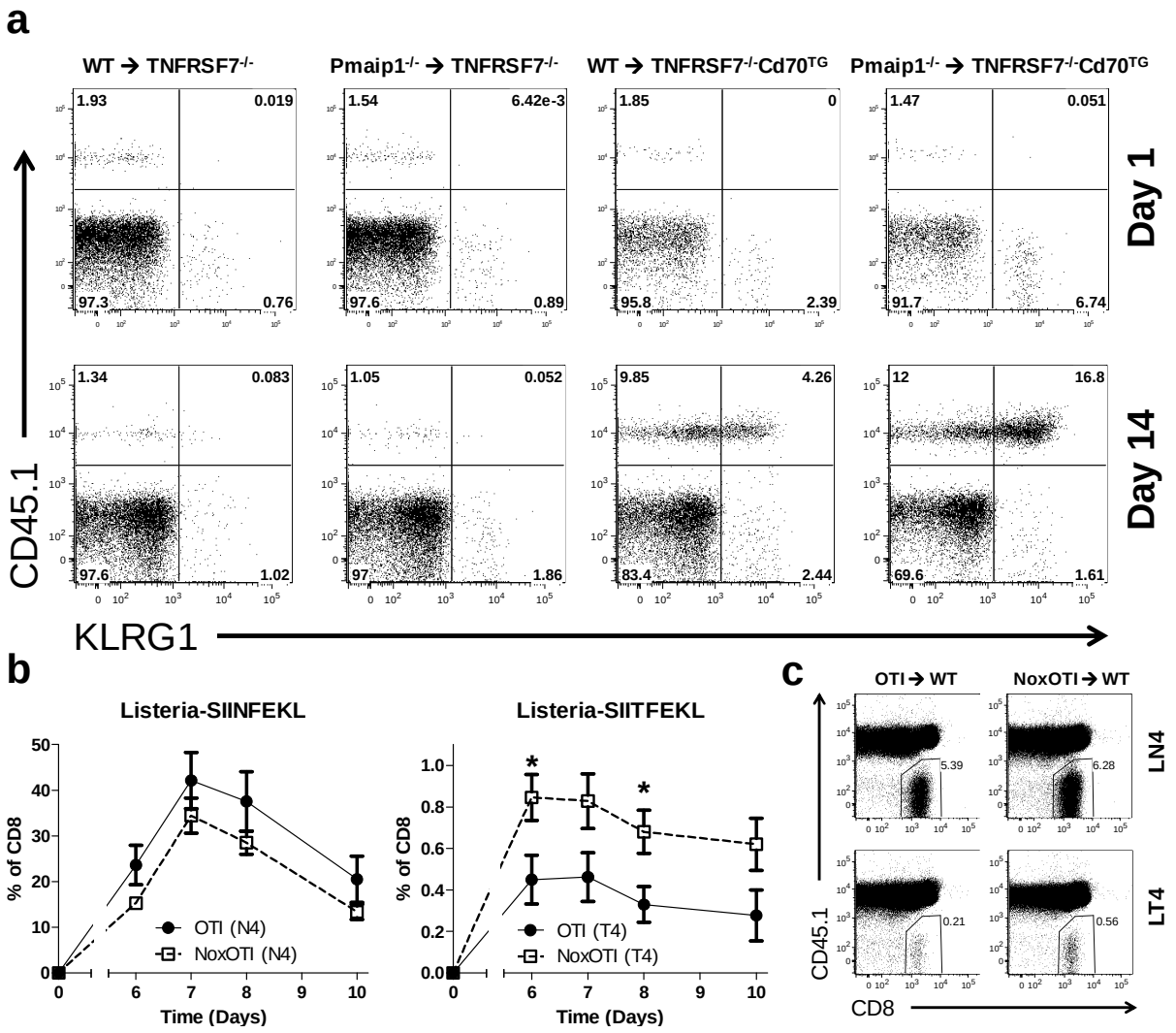

Supplementary Figure S4. **Adoptive transfer of Pmaip1$^{-/-}$ T cells shows enhanced expansion after low affinity triggering.** (**a**) WT (Wt→) and Pmaip1$^{-/-}$ (Pmaip1$^{-/-}$→) T cells (Ly5.1^{+}) were adoptively transferred in TNFRSF7$^{-/-}$ or TNFRSF7$^{-/-}$Cd70^{TG} recipient mice (Ly5.2^{+}). Shown is the phenotypic analysis of adoptively transferred cells under by KLRG1 staining. Cells were gated for CD8^{+}. **b, c**, OT-I and NoxOTI T cells (Ly5.2^{+}) were adoptively transferred in Wild Type recipient mice (Ly5.1^{+}). One day after transfer, recipient mice were infected with Listeria-SIINFEKL (LN4; n=3) or with low affinity Listeria-SIITFEKL (LT4; n=5). (**b**) Shown is the number of donor cells as a fraction the total CD8 T cell pool. Error bars represent SEM. (**c**) Representative FACS plots of total white blood cells 6 days after infection.

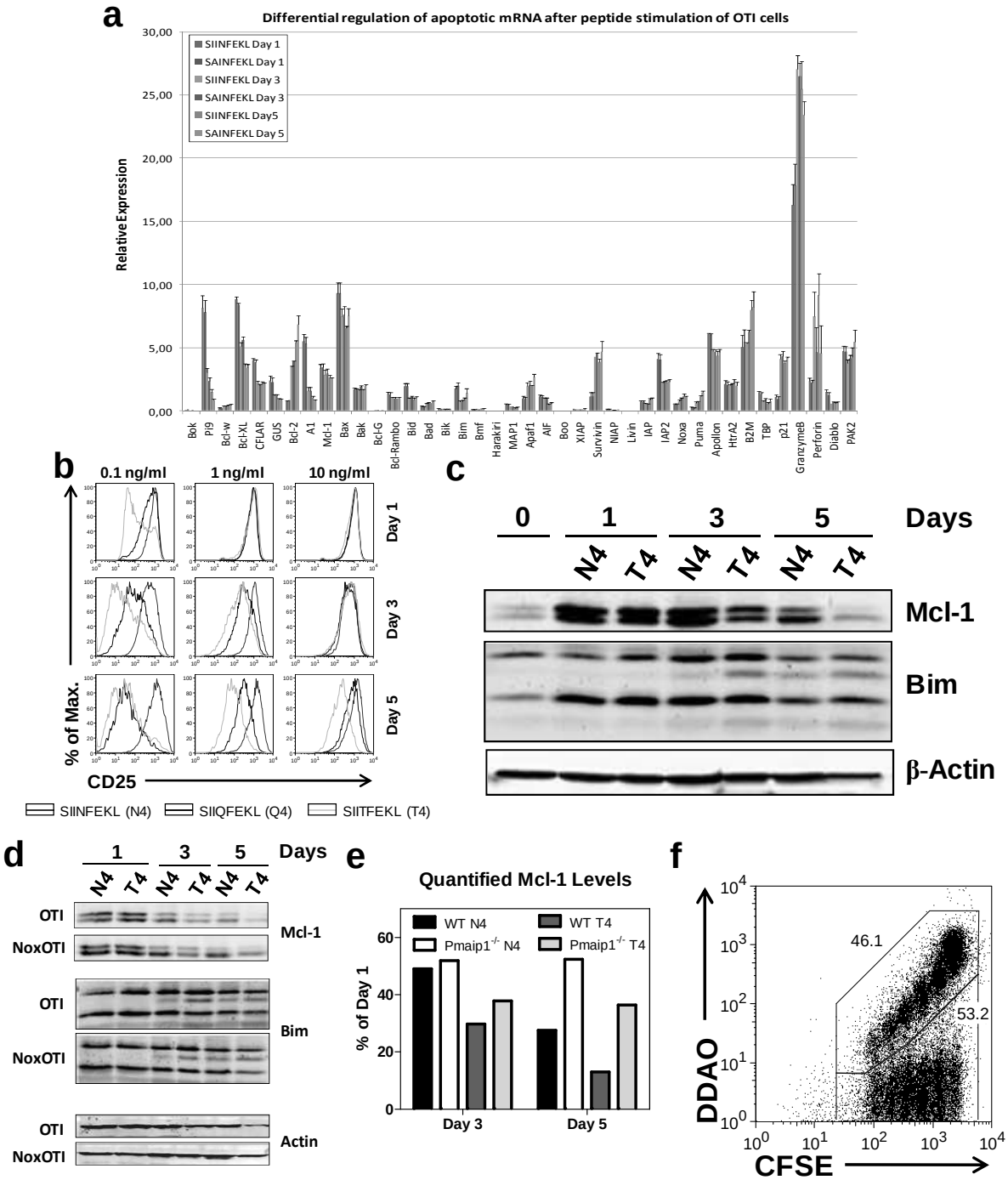

Supplementary Figure S5. Differential apoptotic gene expression in peptide stimulated OT-I T cells a, Expression profile of OT-I T cells stimulated for 1, 3 and 5 days with 10 ng/ml high affinity (SIINFEKL; N4) or low affinity (SAINFEKL; A2) peptides, measured by RT-MLPA. Peaks represent signals relative to the sum of all peaks combined. (n = 3). **b**, Overlays of CD25 expression of purified OT-I T cells stimulated for 1, 3 and 5 days with 0.1, 1 and 10 ng/ml of SIINFEKL (N4), SIIQFEKL (Q4) or SIITFEKL (T4) peptides. **c**, Purified splenic OT-I transgenic T cells were stimulated with 0,1 ng/ml high affinity SIINFEKL (N4) or low affinity SIITFEKL (T4) peptides and apoptotic molecules were analyzed by western blot. Shown is one of three independent experiments with similar results. **d**, Purified splenic OT-I and NoxOTI T cells were stimulated with 0,1 ng/ml high affinity SIINFEKL (N4) or low affinity SIITFEKL (T4) peptides as indicated and apoptotic molecules were analyzed by western blot on designated days. Shown is one of two independent experiments. **e**, Quantification of Mcl-1 expression shown in d. **f**, Representative FACS plot of a mixed OTI/NoxOTI experiment three days after N4 stimulation, in which one population was labeled with DDAO and both with CFSE. DDAO positive and negative cells could be distinguished up to day 3 after stimulation.

Supplementary Table 1.

List of FACS antibodies

Antigen	Antibody clone	Company
CD3ε	145-2C11	BD Biosciences
CD3ε	17A2	BD Biosciences
CD28	37.51	Bioceros B.V.
CD16/32	2.4G2	Bioceros B.V.
B220	RB6-6B2	eBioscience
CD25	PC61.5	eBioscience
CD4	GK1.5	eBioscience
CD4	L3T4	BD Biosciences
CD8	53.6.7	eBioscience
CD44	IM7	eBioscience
CD45.1	A20	eBioscience
CD62L	MEL-14	BD Biosciences
CD69	H1.2F3	BD Biosciences
CD127	A7R34	eBioscience
FoxP3	FJK-16s	eBioscience
F4/80	BM8	eBioscience
GR1	RB6-8C5	BD Biosciences
IFNγ	XMG1.2	eBioscience
IL-2	JES6-5H4	BD Bioscience
IL-10	JES5-16E3	BD Bioscience
IL-17	TC11-18H10.1	eBioscience
PD-1 (CD279)	J43	eBioscience
KLRG1	2F1	eBioscience
Vβ5	MR9-4	BD Biosciences
Vβ6	RR4-7	BD Biosciences
Vβ8.1/8.2	F23.1	BD Biosciences
Vβ8.3	CT11-8C11	eBioscience